SPIN DYNAMICS IN THE PRESENCE OF SPIN-ORBIT INTERACTIONS: FROM THE WEAK TO THE STRONG SPIN-ORBIT COUPLING REGIME

A Dissertation

by

XIN LIU

Submitted to the Office of Graduate Studies of
Texas A&M University
in partial fulfillment of the requirements for the degree of

DOCTOR OF PHILOSOPHY

August 2012

Major Subject: Physics

SPIN DYNAMICS IN THE PRESENCE OF SPIN-ORBIT INTERACTIONS: FROM THE WEAK TO THE STRONG SPIN-ORBIT COUPLING REGIME

A Dissertation

by

XIN LIU

Submitted to the Office of Graduate Studies of
Texas A&M University
in partial fulfillment of the requirements for the degree of

DOCTOR OF PHILOSOPHY

Approved by:

Chair of Committee,	Jairo Sinova
Committee Members,	Artem G. Abanov
	Alexey Belyanin
	Winfried Teizer
	Ohannes Eknoyan
Head of Department,	Edward Fry

August 2012

Major Subject: Physics

ABSTRACT

Spin Dynamics in the Presence of Spin-orbit Interactions: from the Weak to the Strong Spin-orbit Coupling Regime. (August 2012)
Xin Liu, B.S, Nankai University; M.A., Chern Institute of Mathematics
Chair of Advisory Committee: Dr. Jairo Sinova

We study the spin dynamics in a high-mobility two dimensional electron gas (2DEG) system with generic spin-orbit interactions (SOIs). We derive a set of spin dynamic equations which capture the purely exponential to the damped oscillatory spin evolution modes observed in different regimes of SOI strength. Hence we provide a full treatment of the D'yakonov-Perel's mechanism by using the microscopic linear response theory from the weak to the strong SOI limit. We show that the damped oscillatory modes appear when the electron scattering time is larger than half of the spin precession time due to the SOI, in agreement with recent observations. We propose a new way to measure the scattering time and the relative strength of Rashba and linear Dresselhaus SOIs based on these modes and optical grating experiments. We discuss the physical interpretation of each of these modes in the context of Rabi oscillation. In the finite temperature, We study the spin dynamics in the presence of impurity and electron-electron (e-e) scattering in a III-V semiconductor quantum well. Starting from the Keldysh formalism, we develop the spin-charge dynamic equation at finite temperature in the presence of inelastic scattering which provide a new approach to describe the spin relaxation from the weak to the strong spin-orbit coupling (SOC) regime. In the weak SOC regime, our theory shows that when the system is near the SU(2) symmetry point, because the spin relaxation due to DP mechanism is suppressed dramatically, the spin relaxation is dominated by the Elliott-Yafet (EY) mechanism in a wide temperature regime. The non-monotonic

temperature dependence of enhanced-lifetime of spin helix mode is due to the competition between the DP and EY mechanisms. In the strong SOC regime, the our theory is consistent to the previous theoretical results at zero temperature.

DEDICATION

To my family, for their love and support

ACKNOWLEDGMENTS

I would like to express my heartfelt gratitude to Professor Jairo Sinova for mentoring me throughout my academic program. I am grateful that Prof. Sinova gave me such an interesting project to do and this dissertation could not have been written without him. He provided permissive managerial latitude to allow me to be a student, an independent thinker, and a researcher. I also would like to acknowledge Prof. Chia-Ren Hu for his fruitful and interesting discussions, I thank him for introducing many exciting topics of physics. I thank all our current and former group members in Sinova's group for their support, help, and valuable recipes! Thank you all for giving me opinions from different angles. I would like to give special thanks to Mario F. Borunda for his guidance of the numerical programming, wonderful and precious discussions and friendship.

"Thank you" is not enough for my family. My parents love me and support me no matter what I choose to do. My wife, my love and my best friend, always supports and encourages me. My beloved daughter, you lighten my life with so many laughs.

TABLE OF CONTENTS

Page

Page

LIST OF FIGURES

FIGURE Page

FIGURE Page

1. INTRODUCTION

1.1 Spin-orbit interactions in the Modern Physics

The spin-orbit coupling attracts a lot of interests because of its technique application and the importance in the fundamental science. The SOC originates from the special relativity and was assumed to be only interesting for the fundamental science. However, in recent years research in semiconductor based devices has incorporated the spin degree of freedom as a new state variable in novel electronic devices with potential for future applications. The SOI here becomes a key tool to electrically manipulate the spin and realize such devices. SOI is already a key component of metallic spintronics such as AMR (1; 2). Recently, many interests (3; 4; 5; 6; 7; 8; 9) focus on finding an alternative logic device in semiconductors where we use spin, other than charge, to store and transport the information by the electric field. This is very helpful to make the device in a smaller scale where the magnetic field cannot be confined to the so small area. On the other hand, the SOC also crates some new phenomena such as spin hall effect (10; 11; 12; 13; 14) and topological insulators (15; 16; 17; 18; 19; 20; 21; 22) which are very active research fields. These new phenomena are related to the fact that the SOC couples different spin sub-bands, so we have to deal with the multi-band physics. In the topological insulator, the degrees freedom of the bands index forms a parameter space where the property of the crystal is decided by the topology of this parameter space. In the spin hall effect, the effective magnetic field can deflect the electron in the different spin sub bands to the opposite directions. This is like a spin-version of Lorentz force which induces the experimentally observable spin accumulation on the edges of the sample. This provides a possible way to manipulate the spin by the electric field. However, the

This dissertation follows the style of *Physical Review Letters*.

spin-orbit coupling is a two edge sword. It also makes the spin diffuse faster. Therefore it is necessary to study the spin dynamics in the presence of the SOC. Now, let me give physical picture of the spin dynamics in the III-V semiconductor quantum wells such as GaAs. The spin splitting energy due to SOC is the order of several hundred ueV. The Fermi energy in this sample is the order of several meV (23; 24). Therefore, SOC can play a very crucial role of the spin dynamics and transport in the III-V semiconductor devices. The spin precession frequency in this type of material can be up to the order of 0.5 THz (25). In the logic devices, to reduce the power consumption, we need the high mobility semiconductors. The high mobility means the long mean free time. In now days, the electron mean free time of the 2DEG can be as high as the order of 10ps (25). Therefore in a possible spin-based logic device, the spin can finish several periods of precession between two successive momentum scatterings. This is defined as the strong spin-orbit coupling regime. However the standard spin diffusion equation assumes the spin precession angle between two successive momentum scatterings is very small and can be treated perturbatively. So the standard spin diffusion equation does not contain the spin dynamics in the strong SOC regime. Therefore, it is very important to develop a theory to describe the spin dynamics and transport in the strong SOC regime.

2. SPIN DYNAMICS IN THE ZERO TEMPERATURE *

2.1 Introduction

In recent years research in semiconductor based devices has incorporated the spin degree of freedom as a new state variable in novel electronic devices with potential for future applications. The SOI is a key tool to electrically manipulate the spin and realize such devices. However, the SOI is a double-edged sword because it will also induce random spin precession through an angle $\Omega_{so}\tau$ between collisions with impurities, where τ is the electron life time. This is known as the D'yakonov-Perel's(DP) mechanism(26; 27; 28) and dominates the spin relaxation in the technologically important III-V semiconductors.(29) Therefore it is very important to understand fully the DP mechanism for the possible application and further development of spintronics devises. Although the study of DP mechanism in semiconductors in the presence of SOI was initiated long ago, most of the theoretical research (30; 31; 32; 33; 34; 35) focuses on the weak spin-orbit coupling (SOC) regime where $\Omega_{so}\tau \ll 1$. However, as high-mobility 2DEG systems are created, it is now not difficult to reach the strong SOI regime experimentally where $\Omega_{so}\tau > 1$ at low temperatures as long as the mobility is approximately larger than $1.2 \times 10^5 \mathrm{cm}^2/\mathrm{Vs}$.(36) The spin evolution in this regime is observed to be damped oscillations in the uniform (23; 36) and nonuniform spin polarized system,(24; 37; 25) which can not be described by spin-charge drift-diffusion equations derived for the weak SOC regime and lacks a clear theoretical explanation.

Here, we study the spin dynamics theoretically from the weak to strong SOC regime. The method we use is linear response theory.(30; 38; 33) We derive a set of

spin dynamical equations in the uniform spin polarized 2DEG with different SOIs in the presence of the short-ranged impurity scattering. For the experiments we consider, even in the strong spin-orbit coupling regime, it is dominated by neutral impurity or interface roughness scattering, which are short-ranged impurity scattering.(23) The weak localization effect on the spin relaxation (39; 40) is neglected in our work because we consider the spin relaxation in the metallic regime where weak localization effect is small.

We show analytically that for $\Omega_{so}\tau > \frac{1}{2}$ the damped oscillations appear. The decay rate in this case is proportional to $\frac{1}{\tau}$ instead of τ as in the weak SOC regime. The cubic Dresselhaus term is shown to reduce the oscillatory frequency and increase the decay rate in the strong SOC regime. The spin dynamics for non-uniform spin polarization with spatial frequency q in the strong SOC regime is obtained by solving the equations numerically. We discuss these dynamics by using the analogy with Rabi oscillations between two momentum states which are gaped by the SOI. Our results match the experimental observation quantitatively. We also show how to exploit our analysis to create an accurate measurement of the strength of Rashba and linear Dresselhaus SOIs in a 2DEG, hence allowing a full characterization of different device samples which will lead to a more accurate modeling and predictability of the optimal operating physical regimes.

2.2 Model Hamiltonian and density matrix response function

Normally in the 2-D semiconductor heterostructures, we have three kinds of SOIs, namely the linear Rashba (41; 42) term and the linear and cubic Dresselhaus (43) terms. The Hamiltonian takes the form

$$H = \frac{k^2}{2m} + \mathbf{h}(\mathbf{k}) \cdot \hat{\sigma}, \tag{2.1}$$

where $\mathbf{h}(\mathbf{k})$ is the effective magnetic and contains Rashba, linear and cubic Dresselhaus terms which are

$$\mathbf{h}^{R}(\mathbf{k}) = \alpha(-k_y, k_x), \tag{2.2}$$

$$\mathbf{h}^{D_1}(\mathbf{k}) = \beta_1(k_y, k_x), \tag{2.3}$$

$$\mathbf{h}^{D_3}(\mathbf{k}) = -2\beta_3 \cos 2\theta(-k_y, k_x), \tag{2.4}$$

where k_f is the Fermi wave vector. Here we take θ as the angle between the wave vector $\mathbf{k}$ and the [110] direction which is the x axis in our coordinates. The above SOIs split the spin-degenerate bands and dominate the spin dynamics in the 2DEG. The corresponding SOC Hamiltonian and the spin precession frequency Ω_{so} takes the form:

$$H^{so} = (\lambda_1 - 2\beta_3 \cos 2\theta)k_x\sigma_y + (\lambda_2 + 2\beta_3 \cos 2\theta)k_y\sigma_x, \tag{2.5}$$

where $\lambda_1 = \alpha + \beta_1$, $\lambda_2 = \beta_1 - \alpha$.

We derive the spin dynamic equations from the density matrix response function,(38). The spin diffusion is dominated by the pole of the spin-charge diffusion propagator or "diffuson"(30):

$$\mathcal{D} = [1 - \hat{I}]^{-1} \tag{2.6}$$

and

$$\hat{I}_{\sigma_1\sigma_2,\sigma_3\sigma_4} = \frac{1}{2m\tau} \int \frac{d^2k}{(2\pi)^2} G^{A}_{\sigma_3\sigma_1}(k, 0) G^{R}_{\sigma_2\sigma_4}(k + q, \Omega), \tag{2.7}$$

where σ_i is just a number which can be 1 or 2.(30) It is more convenient to write the Eq. 2.7 in a classical charge-spin space

$$I^{\alpha\beta} = \mathrm{Tr}(\sigma_\alpha \hat{I} \sigma_\beta), \tag{2.8}$$

where $\alpha, \beta = c, x, y, z$.(30)

If one calculates the response function by expanding in term of $\Omega_{so}\tau$ to the first order, the spin relaxation behavior obtained by this approximate response function is only valid in the weak SOC regime (33). However, if one calculates the response function exactly without any expansion in the parameter $\Omega_{so}\tau$, this response function can give the spin relaxation in both weak and strong SOC regime. Although A. A. Burkov *et al* (30) give the expression of the spin-charge diffuson in the presence of the Rashba spin-orbit interaction. The authors (30) are interested in finding a spin-charge drift diffusion equation, only applicable in weak SOC regime, and therefore they expanded the expressions in terms of $\Omega_{so}\tau$ to the first order. However they claim that the expression should be useful in the strong SOC regime. Here, we will calculate the diffuson matrix exactly with the genetic SOIs and find the poles of this exact expression.

2.3 Uniform spin polarization

In the case of a uniform spin polarized 2DEG system, i.e. $q = 0$, because the effective magnetic field due to the SOI has inversion symmetry in momentum space, only the diagonal elements of the diffuson matrix are nonzero, which means the spin x, y, z and charge are not coupled to each other. Therefore, when considering the uniform spin polarization along the z direction, only I^{zz} needs to be calculated. First, we neglect the cubic Dresselhaus term which is normally much smaller than

the linear Dresselhaus term. We find the pole of diffusion matrix by solving the equation

$$1 - I^{zz} = 1 - \frac{1 - i\Omega\tau}{\sqrt{((1 - i\Omega\tau)^2 + (\Omega_{so}\tau)^2)^2 - \gamma^2(\Omega_{so}\tau)^4}} = 0, \tag{2.9}$$

where Ω is the frequency of the spin evolution, $\Omega_{so} = 2\sqrt{\alpha^2 + \beta_1^2}k_f$, $\gamma = \frac{2\alpha\beta_1}{\alpha^2+\beta_1^2} = \frac{\lambda_1^2-\lambda_2^2}{\lambda_1^2+\lambda_2^2}$, k_f is the Fermi wave vector and I^{zz} is obtained from the exact angular integration of Eq.(2.7). The details of calculating I^{zz} are shown in the appendix. There are four solutions of Eq(2.9) which take the form

$$\Omega\tau = -i(1 \pm \frac{\sqrt{2}}{2}\sqrt{1 - 2(\Omega_{so}\tau)^2 \pm \sqrt{1 - 4(\Omega_{so}\tau)^2 + 4(\Omega_{so}\tau)^4\gamma^2}}). \tag{2.10}$$

However we note that not all of these solutions give the spin evolution mode observed by the experiments(23; 36). To find the right one, we explore the values of the above four solutions in the limit of weak spin-orbit coupling regime, say $\Omega_{so}\tau = 0$, and write them as

$$\begin{aligned}
\Omega_1\tau &= -i(1 - \frac{\sqrt{2}}{2}\sqrt{1 - 2(\Omega_{so}\tau)^2 + \sqrt{1 - 4(\Omega_{so}\tau)^2 + 4(\Omega_{so}\tau)^4\gamma^2}}) = 0, \\
\Omega_2\tau &= -i(1 - \frac{\sqrt{2}}{2}\sqrt{1 - 2(\Omega_{so}\tau)^2 - \sqrt{1 - 4(\Omega_{so}\tau)^2 + 4(\Omega_{so}\tau)^4\gamma^2}}) = -i, \\
\Omega_3\tau &= -i(1 + \frac{\sqrt{2}}{2}\sqrt{1 - 2(\Omega_{so}\tau)^2 + \sqrt{1 - 4(\Omega_{so}\tau)^2 + 4(\Omega_{so}\tau)^4\gamma^2}}) = -2i, \\
\Omega_4\tau &= -i(1 + \frac{\sqrt{2}}{2}\sqrt{1 - 2(\Omega_{so}\tau)^2 - \sqrt{1 - 4(\Omega_{so}\tau)^2 + 4(\Omega_{so}\tau)^4\gamma^2}}) = -i. \quad (2.11)
\end{aligned}$$

As we know that for the spin relaxation dominated by the DP mechanism, $\Omega\tau \to 0$ when $\Omega_{so}\tau \to 0$ which indicates that only the first mode, Ω_1, in Eq.2.11 gives the right behavior of the spin relaxation, say $\Omega \propto \tau$,(30) in the weak spin-orbit coupling regime. On the other hand, in the strong spin-orbit coupling regime, there is only one

mode observed in the uniform spin-polarized case.(23; 36) Therefore we can conclude that only the first mode in Eq. (2.11) contributes to the spin relaxation. Therefore, the eigenmode of the spin dynamical evolution takes the form

$$i\Omega\tau = \frac{1}{2}\left(2 - \sqrt{2}\sqrt{1 - 2(\Omega_{so}\tau)^2 + \sqrt{1 - 4(\Omega_{so}\tau)^2 + 4(\Omega_{so}\tau)^4\gamma^2}}\right). \tag{2.12}$$

Note that $\gamma \leq 1$ and

$$(1 - 4(\Omega_{so}\tau)^2 + 4(\Omega_{so}\tau)^4\gamma^2) \leq (1 - 2\Omega_{so}^2\tau^2).$$

Therefore, as long as $1 - 4(\Omega_{so}\tau)^2 + 4(\Omega_{so}\tau)^4\gamma^2 < 0$, a non-equilibrium spin polarization will exhibit damped oscillation with respect to time which are depicted in Fig. 2.1.

In the case of $\alpha = 0$ or $\beta_1 = 0$, the eigenmode takes the form

$$i\Omega\tau = \frac{1}{2} - \frac{1}{2}\sqrt{1 - 4\Omega_{so}^2\tau^2}. \tag{2.13}$$

When $\Omega_{so}\tau > 1/2$, the decay rate changes from the exponential decay mode to the damped oscillation mode. The oscillatory frequency in the clean limit, $\tau \to \infty$, is Ω_{so}. Several experiments(23; 36; 24; 37) observe the damped oscillation mode of spin evolution at low temperature. However their analysis did not explain quantitatively when this kind of mode appears but just qualitatively argue that it appears in the regime where $\Omega_{so}\tau > 1$. Our theory agrees with the recent experiment (23) in which the authors observe that when the temperature is above 5 K, the oscillation will disappear. In their system this corresponds to $\Omega_{so}\tau_p^* \approx 0.48$, which is close to our result 1/2. Here τ_p^* is different to the transport scattering time τ_p obtained from the mobility; this difference is due to the Coulomb interaction effect on spin-currents and spin dephasing.(24; 32) This e-e interactions treatment is beyond our paper and will not be discussed in this work. The τ here is corresponding to τ_p^*. When the

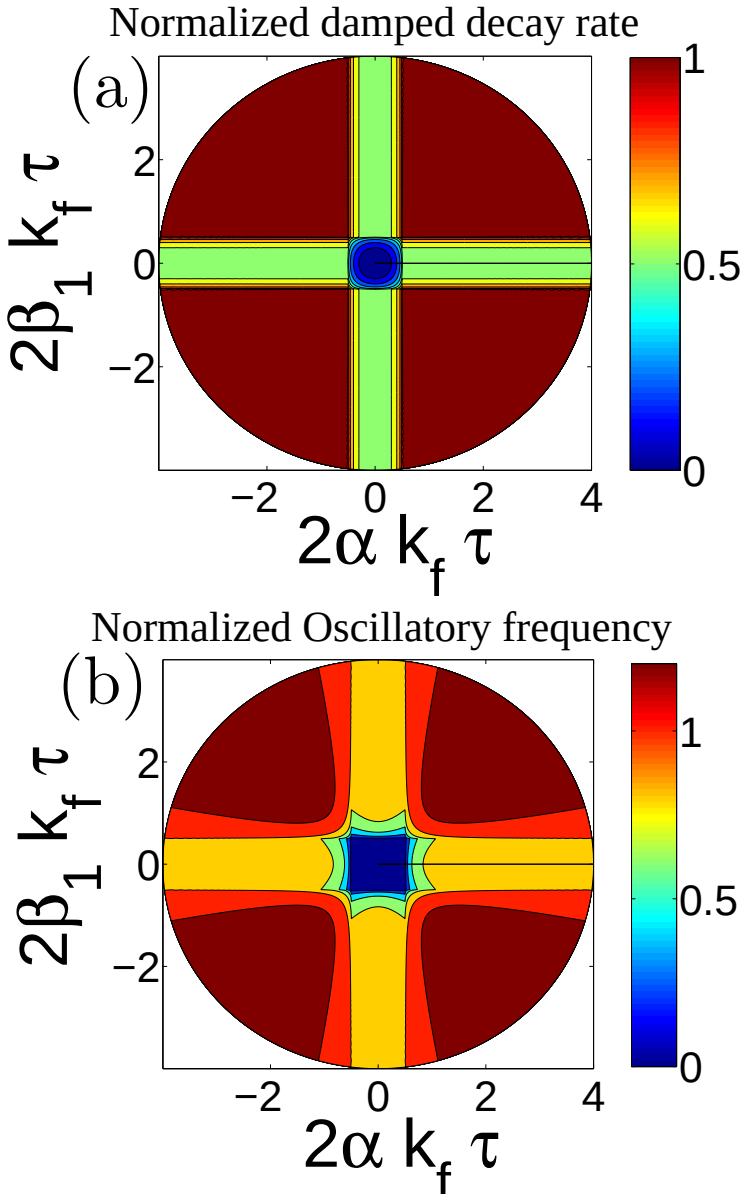

Fig. 2.1. The uniform spin dynamics from the weak to the strong spin-orbit coupling regime in the presence of both Rashba and linear Dresselhaus terms. (a) The normalized exponential decay rate $\Im(\Omega\tau)$ is shown as a function of normalized Rashba and linear Dresselhaus SOI. (b) The nonzero normalized oscillatory frequency, $\frac{\Re(\Omega)}{\Omega_{so}}$, is nonzero whenever $2\alpha k_f\tau \geq \frac{1}{2}$ or $2\beta_1 k_f\tau \geq \frac{1}{2}$.

oscillatory mode appears, the damped decay rate is always equal to $\frac{1}{2\tau}$ when either $\alpha = 0$ or $\beta_1 = 0$. This result matches the recent experiment (36) in which the authors found the decay rates for several different 2DEGs always equals $\frac{1}{1.9\tau}$ when the damped oscillatory mode appears, in agreement with our theoretical result.

As the linear and cubic Dresselhaus terms always coexist, we have to consider the effect of cubic Dresselhaus term on Eq. (2.13). We do this in the simplest case, when Rashba coefficient is zero. In this case, the diffuson matrix element I^{zz} takes the form

$$\begin{aligned} I^{zz} &= \frac{1-i\Omega\tau}{\sqrt{(1-i\Omega\tau)^2+\Omega_{so}^2\tau^2(1+2(\frac{\beta_3}{\beta_1})^2-2\frac{\beta_3}{\beta_1})}} \\ &\quad \times\frac{1}{\sqrt{(1-i\Omega\tau)^2+\Omega_{so}^2\tau^2}} \end{aligned} \tag{2.14}$$

where $\Omega_{so} = 2\beta_1 k_f$ and $\delta = 2\frac{\beta_3}{\beta_1}(1-\frac{\beta_3}{\beta_1})$. The corresponding spin decay rate is

$$i\Omega\tau = 1 - \frac{\sqrt{(1+\sqrt{1-4\Omega_{so}^2\tau^2+2\Omega_{so}^2\tau^2\delta+\Omega_{so}^4\tau^4\delta^2})^2-\Omega_{so}^4\tau^4\delta^2}}{2}. \tag{2.15}$$

Eq. (2.13,2.15) show that the cubic term will increase the exponential decay rate and decrease the oscillatory frequency. To show the effect of the cubic Dresselhaus term, the real(imagine) value of the damped oscillatory frequency when $\beta_3 \neq 0$ is divided by the value when $\beta_3 = 0$. This ratio is ploted in Fig 2.2 with respect β_3/β_1 and $2\beta_1\tau$. When $\frac{\beta_3}{\beta_1} < 0.2$, the effect of the cubic term is very small and can be neglected. In this case, the damped decay rate is always equal to $\frac{1}{2\tau}$ as long as $\Omega_{so} > \frac{1}{2}$ and the oscillatory frequency Ω approach Ω_{so} when $\Omega_{so}\tau \gg 1$. This provides a reliable way to measure the momentum scattering time τ. Further, the strength of the linear

Dresselhaus SOI can be obtained from Eq. (2.13) once we know τ and the oscillatory frequency from the measurements. These will be discussed in a later section.

Now, let us choose $\alpha = \beta_1$ which is a more unique case and gives us the persistent spin helix for special q values.(37; 44; 25) For the uniform spin polarization, the decay rate of the spin satisfies

$$i\Omega\tau = 1 - \sqrt{1 - 2(\Omega_{so}\tau)^2}, \tag{2.16}$$

where $\Omega_{so} = 2\sqrt{\alpha^2 + \beta_1^2}k_f$. The damped oscillation mode will happen when $\Omega_{so}\tau = 2\sqrt{2}\alpha k_f\tau > \sqrt{2}/2$, say $2\alpha k_f\tau > 1/2$ which is the same as the pure Rashba or Dresselhauss case. The oscillating frequency in the clean limit is $\sqrt{2}\Omega_{so} = 4\alpha k_f$ which is the two fold of the frequency for the pure Rashba or Dresselhauss case. On the other hand, as the real part of $i\Omega\tau$ is equal to 1 when damped oscillation mode appear, the damped decay rate is also the two fold of the case of the pure Rashba or Dresselhauss.

2.4 Spin dynamics and Rabi oscillation

Before we discuss the spin dynamics for the nonuniform spin polarization system, let us give a physical explanation of the result we have obtained. We can construct a simple physics picture to describe the spin polarized wave theoretically. Taking the Rashba SOI for example, we define the eigenstates $|\phi_k^a\rangle$ to denote the majority band and the $|\phi_k^b\rangle$ to denote the minority band. The spin of the eigenstate of the SOC 2DEG lies in the $x - y$ plane. The majority electron has opposite spin to the minority electron when they have the same wave vector k. As a result, The spin polarization along the z direction can be obtained by the superposition of the majority and minority bands as

$$\psi_{\uparrow,q} = A[\sum_k e^{(\epsilon-\epsilon_f)^2/4\sigma^2}\frac{1}{\sqrt{2}}(|\phi_k^a\rangle + |\phi_{k+q}^b\rangle)]$$

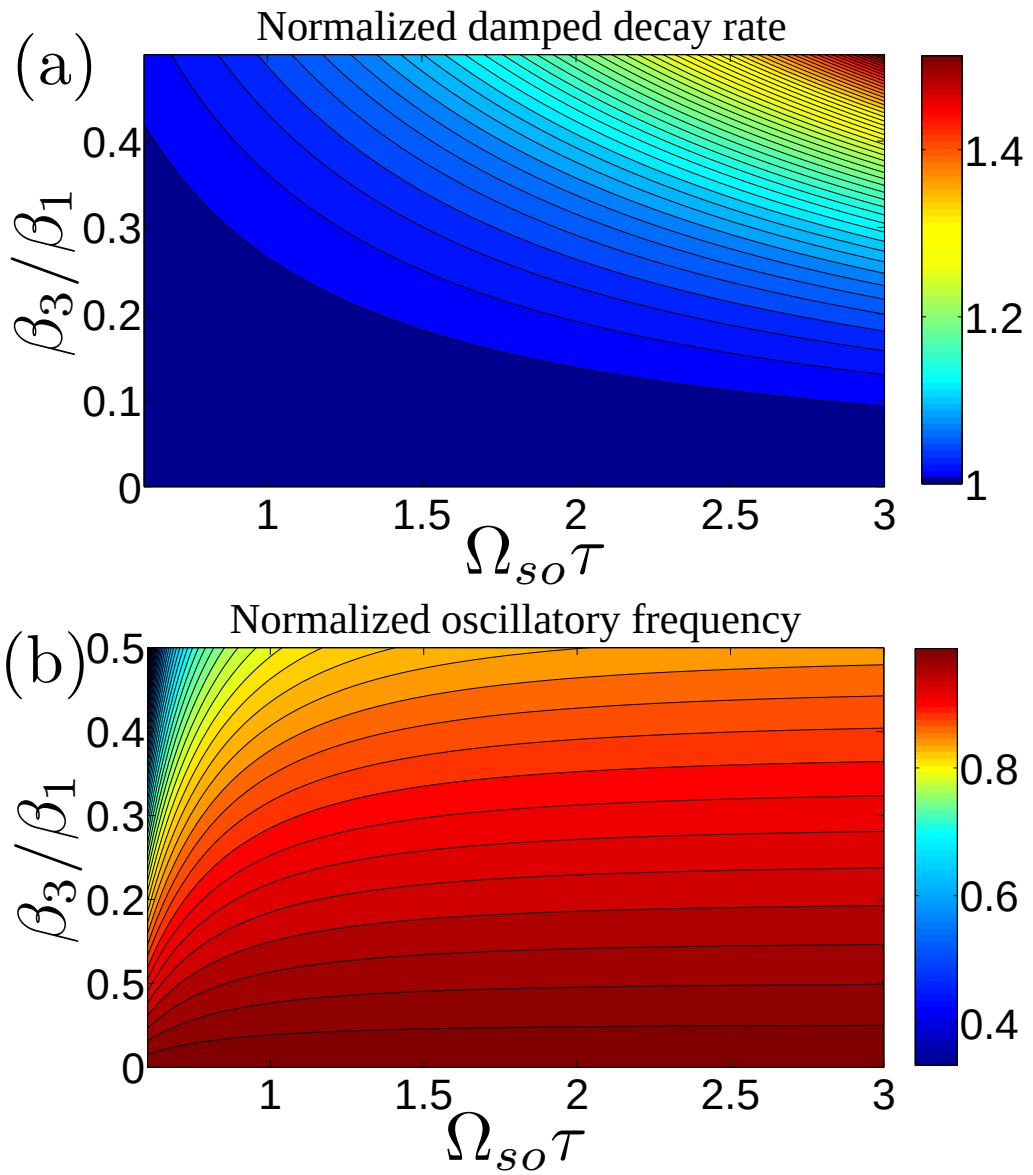

Fig. 2.2. The uniform spin dynamics from the weak to the strong spin-orbit coupling regime in the presence of linear β_1 and cubic β_3 SOI. (a) The normalized exponential decay rate, $\Re(i\Omega\tau)$ is constant when β_3 is zero and slightly larger than $\frac{1}{2}$ when β_3 is nonzero. (b) The nonzero normalized oscillatory frequency, $\Im(i\Omega\tau)$, appear when $\Omega_{so}\tau > \frac{1}{2}$.

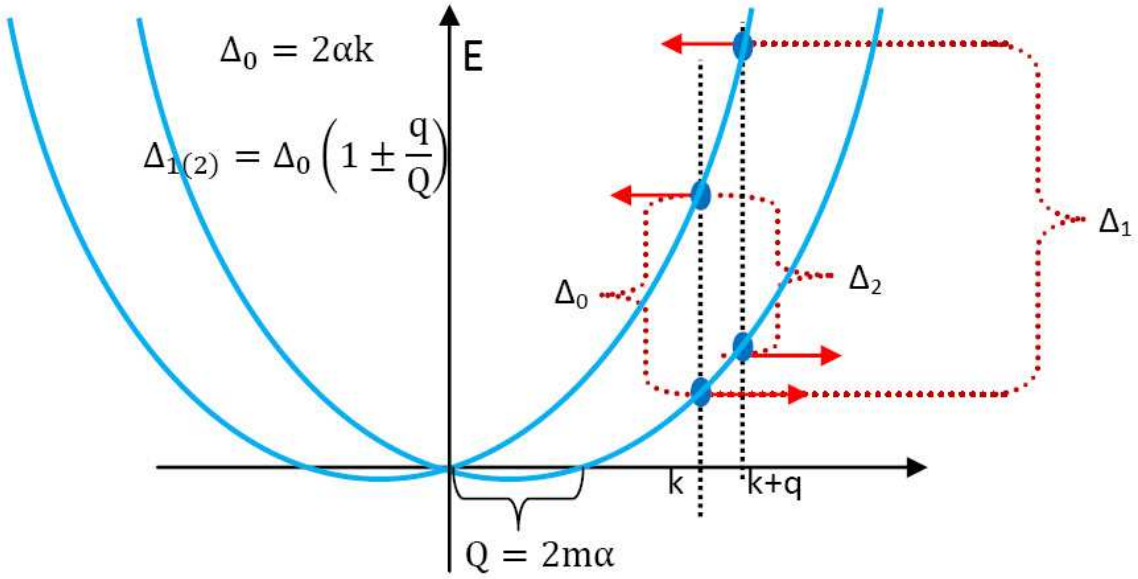

Fig. 2.3. The dispersion relation due to the linear Dresselhaus SOI. The SOI induces the energy gap $\Delta_0 = 2\beta_1 k$ which is the spin precession frequency for the single electron spin. However, when the system is excited to be a spin polarization wave with wave vector q, the spin polarization along the z direction is constructed by the superposition of the two electron with wave vectors k and $k + q$. In this case, the spin precession frequency will be $\Delta_{1(2)} \simeq \Delta_0(1 \pm \frac{q}{Q})$, where $Q = 2m\beta_1$.

$$+ \quad A[\sum_k e^{(\epsilon-\epsilon_f)^2/4\sigma^2}\frac{1}{\sqrt{2}}(|\phi_k^b\rangle + |\phi_{k+q}^a\rangle)], \tag{2.17}$$

where A is the normalization coefficient, $\psi_{\uparrow,q}$ is the wave function of the system with positive spin polarization along z direction with wave vector q and the function $e^{(\epsilon-\epsilon_f)^2/4\sigma^2}$ restrict the spin polarization electrons only in the narrow range $\frac{1}{2\sigma} \ll \epsilon_f$ around the Fermi energy ϵ_f. The expectation value $\langle\psi_{\uparrow,q}|\sigma_z \cos q'x|\psi_{\uparrow,q}\rangle$ is nonzero only when $q' = q$ which confirms that $\psi_{\uparrow,q}$ can describe the spin polarized wave. The energy difference of these two electrons in the first(second) term on the right hand side of Eq. (2.17)is $\Delta_{1(2)}$ as shown in Fig. (2.3). Therefore, $|\psi\rangle$ can be treated as a collective two level system with two Rabi frequencies $\Omega_{1(2)} = \frac{\Delta_{1(2)}}{\hbar}$. For the uniform spin polarization means $q = 0$ and there is only one Rabi frequency $\Omega_0 = \frac{\Delta_0}{\hbar}$ Fig. 2.3. When the system is very clean, our results, Eq.(2.13,2.16), show that the spin evolution is damped oscillation and the oscillatory frequency is the Rabi frequency. It is a little surprising that when $\alpha = \beta$, although the SOC gap Δ_0 is not a constant, the oscillatory frequency is corresponding to the maximum splitting energy $4\alpha k_f$ instead of the average splitting energy $2\sqrt{2}\alpha k_f$. In the weak SOC regime, the disorder is so strong that the splitting energy due to the SOI is completely submerged in the broadening of the band $\frac{\hbar}{\tau}$. Therefore, the spin polarization just exponential decays. For the non-uniform spin polarization case, since there are two Rabi oscillation frequencies Ω_1 and Ω_2, we expect to have two damped oscillatory modes in the clean system corresponding to energy differences Δ_1 and Δ_2 respectively in Fig. 2.3.

2.5 Non-uniform spin polarization

In the case of the non-uniform spin polarized 2DEG, the initial state is a spin wave with wave vector q, the momentum $\mathbf{k}$ is coupled to $\mathbf{k} + \mathbf{q}$ which makes the center of the Fermi sea be shifted to near $\mathbf{q}$. the average magnetic field is nonzero and the off diagonal elements of the diffusion matrix appear to couple the different

spin component. When only considering the Rashba or linear Dresselhaus SOI, our numerical calculation does have two kinds of spin dynamical modes which are shown in Fig.(2.4,2.5).

The two damped oscillatory mode and their oscillatory frequency satisfy our expectation based on the Rabi oscillation viewpoint. When q increases, the Rabi frequency of the faster mode always increases which makes the damped oscillatory mode appear even when $\Omega_{so}\tau < \frac{1}{2}$. This means we can expect to observe the oscillation for the nonzero spin polarization at higher temperature than for the uniform spin polarization. In Ref (23) where the spin polarization is uniform, the damped oscillatory mode appears below 5K. On the other hand in Ref (24), where the spin polarization is nonuniform, the damped oscillatory mode appears below 50K. The material, Fermi energy and mobility in these two papers are similar. This seems support our Rabi oscillation viewpoint. For the slow oscillatory mode, when q is around Q, the corresponding Rabi frequency Ω_2 is around 0 which means the spin precession is very slow. Because the Rabi frequencies is much smaller than $\frac{1}{\tau}$, the spin polarization just decays exponentially and the exponential decay rate has its minimum in this regime when q is around Q .

A particular case is when $\alpha = \beta_1$ and $\beta_3 = 0$. The analytical solutions of these two modes can be obtained by finding the poles of Eq. (20) of Ref (44) and have the form

$$i\Omega\tau = 1 - \sqrt{1 - (\Omega_{so}\tau)^2(1 \pm \frac{q}{Q})^2} \tag{2.18}$$

where $Q = 4m\alpha$. At $q = Q$, the Rabi frequency of the slower mode is zero for all of the electron momentum k. On the other hand, the spin y is a good quantum number for all the electron states which means the spin independent disorder will never couple the two electrons in different bands with different spin directions. Therefore, the Rabi frequency of the slower mode is still exactly zero even in the presence of the spin independent disorder no matter how strong it is. As a result, the spin along the z-

direction will never precess and has infinite long life time. This provides another way to understand the persistent spin helix.(37; 25) However, the cubic Dresselhaus SOI induces band transition in the presence of spin independent impurities and makes the spin life time finite.(33) When $\alpha \neq \beta_1$, even at $q = Q$, the gap of the two electrons with momentum k and $k+q$ in different spin bands is dependent on k and fluctuates around the average value of the gap. The average value of the Rabi frequency of the slower mode is small but not zero. Therefore the spin relaxation can not be exactly suppressed. However if the average value of the gap is much larger than the fluctuationk, normally when $q \gg Q$, the spin relaxation can be described by Eq. (2.18) well for arbitrary combination of α and β_1.

2.6 Proposed experiments

The spin dynamics in the strong SOC regime have several special characters which can be used in experimental measurements.

Momentum scattering time τ_p^*: In the spin dynamics, the Coulomb interaction plays an important role in determining the momentum scattering time τ_p^* (45; 46). This is quite different to the charge transport case where electron-electron(e-e) interaction will not change the ensemble momentum scattering τ_p which determines the electron mobility. This difference is called spin Coulomb drag (SCD). In previous experimental work, SCD was observed through the spin diffusion coefficient $D_s = \frac{1}{2} v_f^2 \tau_p^*$ by fitting the spin decay rate in the weak SOC regime. Here, we provides a way to observe SCD in the strong SOC regime by directly measuring the momentum scattering time τ_p^*. Based on Eqs. (2.13,2.15), when only Dresselhaus SOI is presented, the damped decay rate is always almost equal to 1/2 as long as $\frac{\beta_3}{\beta_1} < 0.2$ which is easily realized in experiments.(36; 25)

The strength of SOIs: Here, we would like to emphasize that $2\beta_1 k_f \tau = \frac{1}{2}$ is a very important case and is corresponding to the transition point between pure exponential decay mode and damped oscillatory mode. The decay rate at this point is not only

equal to $\frac{1}{2\tau}$, but also equal to $\frac{1}{2\beta_1 k_f}$ when $\alpha = 0$. This means that at this point we can obtain the strength of linear Dresselhaus SOI from the spin polarization decay rate. When $2\beta_1 k_f \tau = \frac{1}{2}$, we can increase the Rashba SOI by adding a gate voltage. As long as $0 < \alpha < \beta_1$, according to Eq. (2.12), the spin evolution is still decay exponentially and the decay rate is $(1 - \frac{\sqrt{2}}{2}\sqrt{1 - 2(\Omega_{so}\tau)^2})/\tau$ where $\Omega_{so} = 2\sqrt{\alpha^2 + \beta_1^2} k_f$ which gives us the strength of Rashba SOI.

2.7 Conclusion

We have discussed the spin dynamics in the strong spin-orbit coupling regime. We describe quantitatively the special characters of the damped oscillatory mode in this regime. We also compare our result to the previous experimental data and find they match very well. Based on our theoretical results, a reliable way is proposed to measure the Rashba and Dresselhaus coefficients and electron momentum scattering time which is not corresponding to the mobility due to the Coulomb interaction. Furthermore, we find that the spin dynamics in the 2DEG can be treated as a collective two level system. This helps us semi-quantitatively understand the spin dynamics in the strong spin-orbit coupling regime. For the nonzero spin polarization case, we predict that there exist double damped oscillatory modes at large q and explain the persistent spin helix mode from the Rabi oscillation point of view.

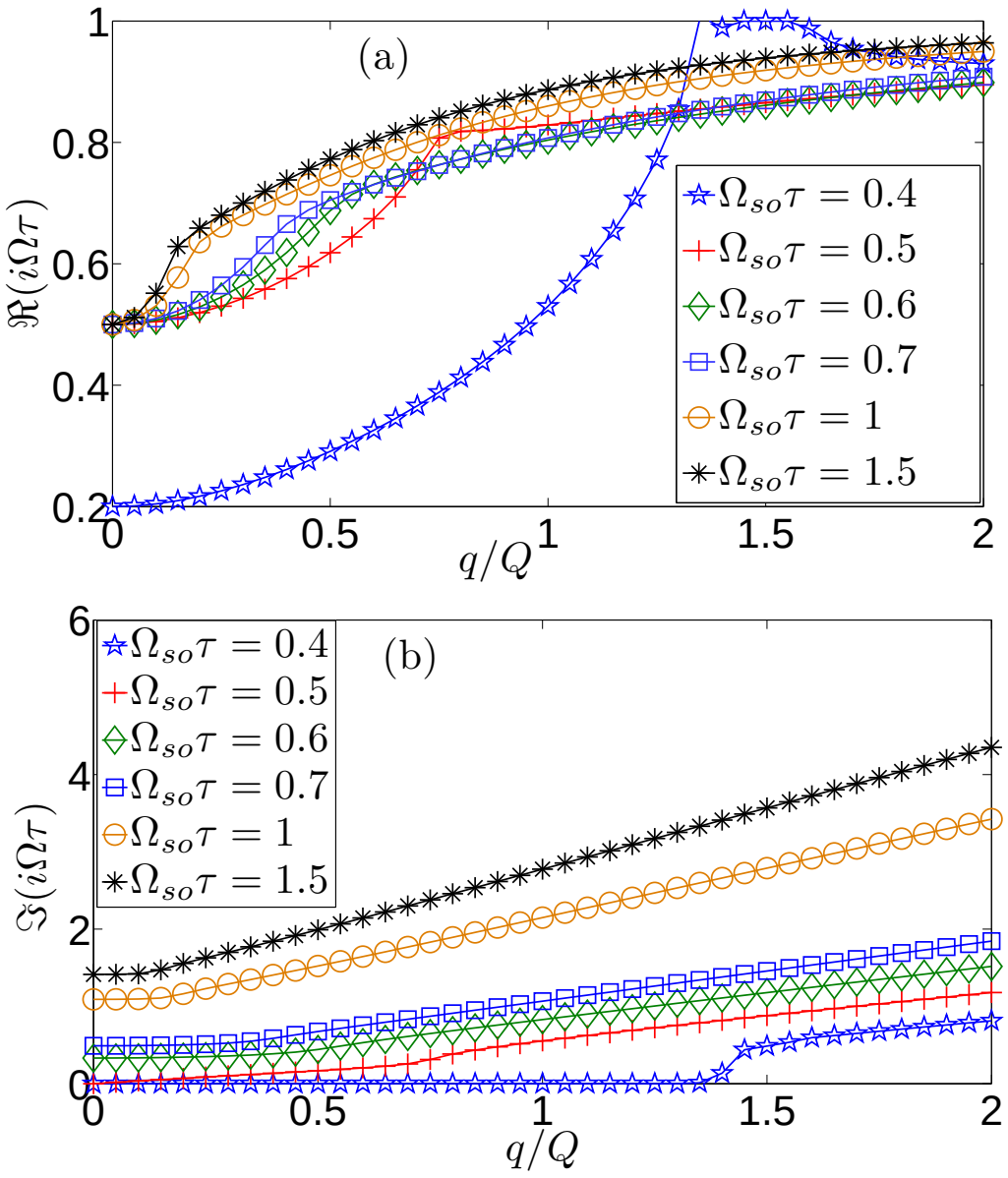

Fig. 2.4. The fast oscillatory mode of the nonuniform spin dynamics in the strong SOC regime when the system only has bulk inversion asymmetry. (a) The normalized exponential decay rate, $\Re(i\Omega\tau)$ increase with increasing q and approach to one at large q. (b) The nonzero normalized oscillatory frequency, $\Im(i\Omega\tau)$, increases linearly at large q, the slope is close to $\Omega_{so}\tau$ and its value approaches $\Omega_{so}(1+\frac{q}{Q})$ where $Q = 2m\beta_1$

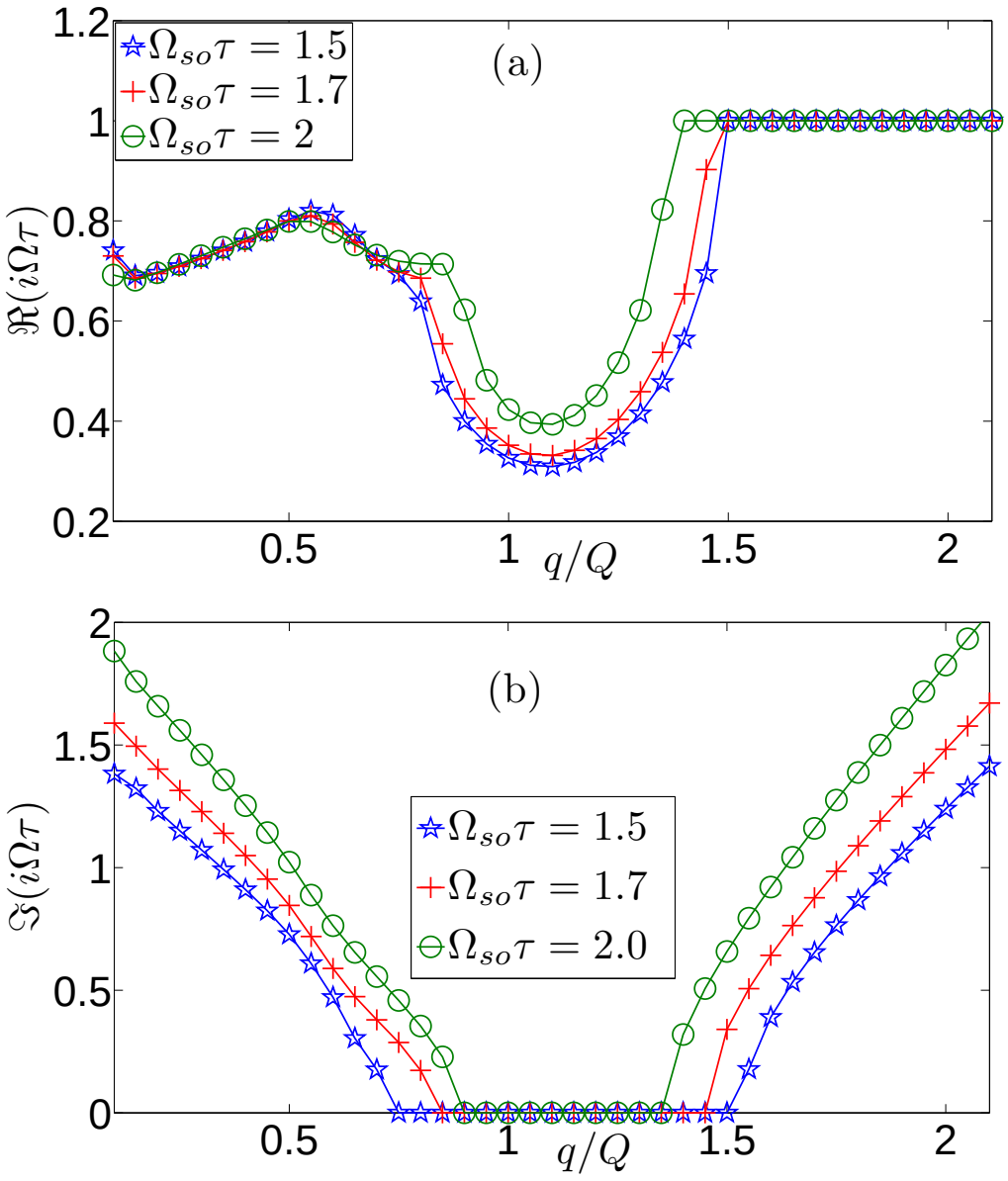

Fig. 2.5. The slow oscillatory mode of the nonuniform spin dynamics in the strong SOC regime when the system only has bulk inversion asymmetry. (a) The normalized exponential decay rate, $\Re(i\Omega\tau)$ has a minimum around $q = Q$ and approach to one at large q. (b) The nonzero normalized oscillatory frequency, $\Im(i\Omega\tau)$ is always zero when q is around Q and increases linearly at large q. The slope is close to $\Omega_{so}\tau$ and the value approaches $\Omega_{so}(1-\frac{q}{Q})$ at large q where $Q = 2m\beta_1$.

3. SPIN DYNAMICS IN THE FINITE TEMPERATURE

3.1 Introduction

Spin-orbit coupling (SOC) plays a very important role in developing the spin-based new electronic devices, say spintronics, because it provides a possible way to manipulate spin by the pure electric mean. Obviously a long spin life time and a strong SOC are desired to store, transport and manipulate information in these types of devices. However, the SOC is a double-edged sword. While a purely electronic manipulation of spin by SOC can make the device in a smaller scale with a lower power consumption, the strong SOC generally also induces fast spin relaxation. Here, the strong SOC is defined as $\Omega_{so}\tau > 1$ where Ω_{so} is the spin precession frequency due to the SOIs and τ is the momentum scattering time. Therefore a center issue of the spintronics is to find the balance between the advantage and disadvantage of the SOC. Recently, this balance is discovered in the III-V semiconductor quantum well when the Rashba SOC strength is equal to the linear Dresselhaus SOC strength. In this system, there exists a spin helical mode (SHM) with an infinite life time (47) without considering the cubic Dresselhaus SOC. When accounting the cubic Dresselhaus SOC, the life time of the SOC enhanced SHM becomes finite but is still two orders longer (25) than the spin life time in the presence of the general spin-orbit interactions. This SHM is verified experimentally and the maximal life time of this SHM is detected at 75 K (25). Further decreasing the momentum scattering time by increasing the temperature will decrease the life time which seems to violate the spin relaxation dominated by the D'yaknov-Perel mechanism. On the other hand, the experimental observations (23; 24; 25) indicated that the e-e interaction is the key to understand the temperature dependence of the spin dynamics in the presence of the SOIs. The momentum of a single electron can be randomized by the impurity scattering, e-ph interaction and e-e interaction. The rate of this randomization is depicted by the life time τ of the electron which can be written as

$\frac{1}{\tau} = \frac{1}{\tau_{imp}} + \frac{1}{\tau_{e-ph}} + \frac{1}{\tau_{e-e}}$. where $\tau_{imp(e-ph,e-e)}$ is the momentum scattering time due to the impurity (electron-phonon, e-e) scattering. The life time τ of the electron means the average time of the electron stay in a particular momentum eigenstate. The e-e scattering time in the 2DEG system has been theoretically discussed very well(48). However it is not easy to be detected in the experiments. In the most system with parabolic momentum dependent spectrum, the life time of the electron is often related to the charge current conductivity by the Einstein relation $\sigma = \frac{e^2 v_f^2}{2} D(E_f)\tau$ where v_f is the Fermi velocity and $D(E_f)$ is the density of state at the Fermi surface. However, as the e-e interaction conserves the net momentum of the system, therefore the life time τ in the Einstein relation does not contain the e-e scattering time which indicates that the charge current is not affected by the e-e interaction. As a result, we can not observe the e-e scattering time by measuring the conductivity and using the Einstein relation. In the last twenty years, the increasing interests in developing the electronic device based on spin impel the physicists to focus on the spin transport. It was widely assumed that the spin current is unaffected by the e-e interaction like the charge current because spin and charge share the same carrier. As a result, according to the generalized Einstein relation of spin current and spin diffusive constant, the e-e interaction also should not affect the spin dynamics. However, I. D'Amico and G. Vignale (49) first pointed out theoretically that the assumption is not valid and the e-e interaction provides the additional friction-like force to the spin current which is named as spin Coulomb drag (49). Lately this theory was confirmed experimentally (24) by the nonuniform spin polarization dynamics. On the other hand, M. A. Brand *et al.* (23), found that they have to put the e-e interaction in their numerical simulation to fit their temperature behavior of the uniform spin polarization dynamics they observed experimentally. These facts demonstrate that the spin dynamics and the spin current do feel the e-e interaction in contrast to the charge current.

Here we develop a consistent microscopic approach based on the quantum Boltzmann equation (QBE) (50) to fully understand the temperature dependence of the spin relaxation in the n-doped III-V semiconductor quantum well by incorporating the e-e interaction. We provide a new way to convert the QBE to the spin-charge density equation which generalize the zero temperature spin-charge dynamic equation (31) to the finite temperature in the presence of e-e inelastic scattering. The momentum scattering time appearing in the spin dynamics is shown to be dominated by the e-e interaction at finite temperature. Both DP and EY mechanisms are derived in the frame of the quantum kinetic equation. The non-monotonic temperature dependence of the enhanced-lifetime of the SHM is shown be the result of the competition between D-P and E-Y mechanism. Our theory is also consistent to the theoretical prediction of the spin relaxation in the strong SOC limit (44; 51). In the appendix B.2, the vanishing e-e interaction in the charge current is naturally derived when converting the QBE to the current equation.

Our paper is constructed as follows: In Sec. 3.2, we introduce quantum kinetic equation (QKE) of the Keldysh Green's function in the presence of the three types of the SOIs in the III-V 2DEG. The e-e interaction is included in the collision integral of the QKE and shown to dominate the momentum scattering time at finite temperature Fig. 3.2. We generalize spin-charge kinetic equation from the zero temperature limit (31) to the finite temperature in the presence of the inelastic scattering.

In Sec. 3.3, we focus on the temperature dependence of enhanced-lifetime of the SHM near the SU(2) symmetry point. The enhanced-lifetime of SHM (47) is observed to be non-monotonically dependent on the temperature (25) which seems to conflict the theoretically prediction that based on the DP spin relaxation mechanism, the lifetime of the SHM should increase monotonically with increasing the temperature. We discuss the thermal average of the SOIs strength which is shown to be almost unchanged from 0K to 100K. Therefore the increasing the thermal average of the cubic Dresselhaus strength is not strong enough to compete the de-

crease of the momentum scattering time and induce the non-monotonic temperature dependence of the enhanced-lifetime of the SHM. Therefore we further discuss the EY mechanism in the presence of the e-e interaction. By adding the EY mechanism in the thermal averaged spin-charge dynamic equation, we show quantitatively that the non-monotonic temperature dependence of the enhanced-lifetime of the SHM is the result of the competition of the EY and DP spin relaxation mechanism.

In Sec. 3.4, we reproduce the spin relaxation eigenmodes in the presence of the different SOIs which confirm that our method is also valid in the strong SOC regime.

3.2 The quantum kinetic equation for the 2DEG with the general SOI

The non-equilibrium spin polarization can be described by the Keldysh formalism (50). This formalism was used in the noninteracting system with the short range disorder and in the presence of the weak Rashba spin-orbit interaction (SOI) (31) or the equal magnitude of Rashba and linear Dresselhaus SOIs with zero cubic Dresselhaus SOI (44). However, when considering the temperature dependence of the spin life time, we have to generalize this method to the interacting system with the general SOIs. Here, we mainly focus on the 2DEG in the quantum well such as GaAs/AlGaAs (23; 24; 37; 25).

In the 2-D semiconductor heterostructures, the Hamiltonian takes the form

$$H = \frac{k^2}{2m} + \mathbf{b}(\mathbf{k}) \cdot \hat{\boldsymbol{\sigma}}, \tag{3.1}$$

where $\mathbf{b}(\mathbf{k})$ is the effective magnetic field and contains three types of SOIs, namely the linear Rashba (41; 42) SOI and the linear and cubic Dresselhaus (43) SOIs which take the form

$$\mathbf{b}^R(\mathbf{k}) = \alpha(-k_y, k_x), \tag{3.2}$$

$$\mathbf{b}^{D_1}(\mathbf{k}) = \beta_1(k_y, k_x), \tag{3.3}$$

$$\mathbf{b}^{D_3}(\mathbf{k}) \;=\; -2\beta_3 \cos 2\theta(-k_y, k_x), \tag{3.4}$$

where k_F is the Fermi wave vector. Here we take θ as the angle between the wave vector $\mathbf{k}$ and the [110] direction which we refer to be the local x axis in our coordinates. The above SOIs split the spin-degenerate bands and dominate the spin dynamics in the 2DEG. The corresponding SOC Hamiltonian takes the form:

$$\hat{H}_{so} \;=\; \lambda_1 k_x \sigma_y + \lambda_2 k_y \sigma_x = b_y \sigma_y + b_x \sigma_x, \tag{3.5}$$

where $\lambda_1 = \alpha + \beta_1 - 2\beta_3 \cos 2\theta$, $\lambda_2 = \beta_1 - \alpha + 2\beta_3 \cos 2\theta$. The retarded (advanced) Green's function of Hamiltonian Eq. 3.1 takes the form

$$G^{R(A)}(E,k) = \frac{(E - \frac{k^2}{2m})\sigma_0 + \boldsymbol{b}(\boldsymbol{k}) \cdot \boldsymbol{\sigma}}{(E - \frac{k^2}{2m} \pm i\delta)^2 - b_{so}^2}. \tag{3.6}$$

The nonequilibrium state of the system can be described by introducing the contour-ordering Green's function in the Keldysh space as

$$\hat{G}(1,2) = \begin{pmatrix} G^R(1,2) & G^K(1,2) \\ 0 & G^A(1,2) \end{pmatrix}, \tag{3.7}$$

where 1 and 2 stand for the condensed notation $1 = (\boldsymbol{x}_1, s_{z1}, t_1)$.

In the presence of the general SOIs, the kinetic part of the quantum Boltzmann equation has the form (52)

$$\begin{aligned} &\partial_T G^K + \frac{1}{2}\{\hat{\mathbf{V}}, \cdot \nabla_{\mathbf{R}} G^K\} + i[\mathbf{b}(\mathbf{k}) \cdot \boldsymbol{\sigma}, G^K] \\ =\; & -i\left[(\Sigma^R G^K - G^K \Sigma^A) - (G^R \Sigma^K - \Sigma^K G^A)\right], \end{aligned} \tag{3.8}$$

where $\hat{V} = \frac{\partial H}{\partial k}$, $[\cdots, \cdots]$ and $\{\cdots, \cdots\}$ stand for commutation relation and anti-commutation relation respectively, and Σ^R, Σ^A and Σ^K are the retarded, advanced

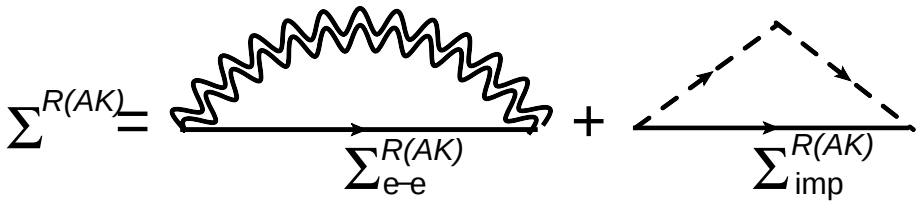

Fig. 3.1. The two self energy we consider in this work. The double wiggle in the first diagram is the effective e-e interaction in the random phase approximation (RPA). The dashed line in the second diagram represents the impurity scattering.

and Keldysh self energy and the corresponding Feynman diagrams are shown in Fig. 3.1. The self energy of the e-e interaction have the more complicated forms (53)

$$\begin{aligned}\Sigma_{ee}^{R(A)} &= \underline{G}^K \circ D^{R(A)} + \underline{G}^{R(A)} \circ D^K, \\ \Sigma_{ee}^{K} &= (\underline{G}^R - \underline{G}^A) \circ (D^R - D^A) + \underline{G}^K \circ D^K, \end{aligned} \tag{3.9}$$

where the symbol $\circ$ denotes integration over all internal energies and momenta, $D^{R(AK)}$ are the full dressed propagator of Coulomb interaction (53) and $\underline{G}^{R(AK)}$ is the electron Green's function in the self energy diagram Fig 3.1 and its energy and momentum is denoted as E' and k' respectively. The underline is to tell its difference to $G^{R(AK)}$ which is the electron Green's function out of the self energy. In the limit $t_1 = t_2$ and $\mathrm{x}_1 = \mathrm{x}_2$, $G^K(t_1 = t_2, \mathrm{x}_1 = \mathrm{x}_2) = 1 - 2\hat{\mathrm{n}}(\mathrm{x}, \mathrm{t})$ where $\hat{n}(x,t) = \psi^\dagger(x,t)\psi(x,t)$ is the electron density operator.

3.2.1 Collision integral of e-e interaction

The collision integral of the impurity scattering has been well established (31). Therefore we will focus on the e-e interaction in the collision integral. The first e-e scattering term has the form

$$\begin{aligned} & \Sigma^R_{ee} G^K - G^K \Sigma^A_{ee} \\ = \; & \left(\underline{G}^K \circ (D^R - D^A) + (\underline{G}^R - \underline{G}^A) \circ D^K \right) G^K . \end{aligned} \tag{3.10}$$

The Keldysh Green's function can be written as $G^K = G^K_0 + \delta G^K$ where $G^K_0(\delta G^K)$ is the Keldysh Green's function of the equilibrium (nonequilibrium) part. The terms containing the first order of δG^K and $\delta \underline{G}^K$ in Eq. 3.10 has the form

$$\begin{aligned} & \left(\underline{G}^K_0 \circ (D^R - D^A) + (\underline{G}^R - \underline{G}^A) \circ D^K \right) \delta G^K \\ & + \delta \underline{G}^K_0 \circ (D^R - D^A) G^K_0 \\ = \; & \frac{i}{\tau_{ee}} \delta G^K + \delta \underline{G}^K \circ (D^R - D^A) G^K_0 . \end{aligned} \tag{3.11}$$

where (53)

$$\begin{aligned} \frac{1}{\tau_{ee}} &= \left(\underline{G}^K_0 \circ (D^R - D^A) + (\underline{G}^R - \underline{G}^A) \circ D^K \right) \\ &= \int \frac{dE'}{2\pi} \frac{d^2k'}{(2\pi)^2} (D^R - D^A)(\underline{G}^R - \underline{G}^A) \\ &\quad \times \left(\tanh(\frac{E'}{2k_bT}) + \coth(\frac{\omega}{2k_bT}) \right) , \end{aligned} \tag{3.12}$$

where $\omega = E - E'$. Similar, the nonquilibrium collision integral in the second term on the right hand side of the Eq. 3.8 can be written up to the first order of $\delta \underline{G}^K$ as

$$G^R \delta\Sigma^K - \delta\Sigma^K G^A = \delta \underline{G}^K \circ D^K (G^R - G^A) \tag{3.13}$$

Substituting Eq. 3.11,3.12,3.13 to the right hand side of Eq. 3.8, the nonquilibrium e-e collision integral has the form

$$I_{ee}(\delta G^K, \delta \underline{G}^K) = I_{ee}(\delta G^K) + \underline{I}_{ee}(\delta \underline{G}^K), \tag{3.14}$$

where

$$\begin{aligned} I_{ee}(\delta G^K) &= \left(\underline{G}_0^K \circ (D^R - D^A) + (\underline{G}^R - \underline{G}^A) \circ D^K\right) \delta G^K \\ &= i\frac{1}{\tau_{ee}} \delta G^K \end{aligned} \tag{3.15}$$

and

$$\begin{aligned} \underline{I}_{ee}(\delta \underline{G}^K) &= \delta \underline{G}^K \circ \left[(D^R - D^A) G_0^K + D^K (G^R - G^A)\right] \\ &= \delta \underline{G}^K \circ (D^R - D^A)(G^R - G^A) \\ &\quad \times \left(\tanh(\frac{E}{2k_bT}) + \coth(\frac{\omega}{2k_bT})\right) \end{aligned} \tag{3.16}$$

It is noted that $\underline{I}_{ee}$ has the similar integrand with that in calculating the momentum scattering time of e-e interaction shown in Eq. 3.12.

Unlike the case of only considering impurity scattering (31; 44), since the collision integral, the right hand side of Eq. 3.8, contains the inelastic e-e scatterings which may scatter the electron to different energy states and make the collision integral of the right hand side of quantum kinetic equation Eq. 3.8 more complicated. Therefore we first give a brief discussion of the e-e interaction in the 2DEG. Because the spin splitting energy Δ_{so} is much smaller than the Fermi energy $\epsilon_F = 400$K, say $\Delta_{so}/\epsilon_F \ll 1$ (25), the screening of the Coulomb interaction in this SOC system is treated to be the same as in the non-SOC system. The inverse screening length in the two dimensional system has the form (48)

$$\kappa_d = \frac{2\pi e^2 N_0}{\epsilon_0}, \tag{3.17}$$

where N_0 is the density of state at the Fermi surface, e is the electron charge and ϵ_0 is the dielectric constant in the vacuum. For the GaAs/AlGaAs, $N_0 = \frac{m^*}{\pi\hbar^2}$ where $m^* = 0.065m_0$ (54) is the effective mass of the electron in the quantum well and m_0 is the mass of electron in the vacuum. In this case, $\kappa_d \approx 3.08 \times 10^8$ cm^{-1} which is much larger than the Fermi wave length $k_F = \sqrt{2\pi n_0} = 2.24 \times 10^6$ cm^{-1} where $n_0 = 8 \times 10^{11}$ cm^{-2} is the density of electrons (25). Therefore the Coulomb interaction is strongly screened in the 2DEG and we can treat the e-e interaction as the angle independent scattering. On the other hand, the peak of the enhanced-life time of the SHM happens around 75 K (25) which is much smaller than the Fermi temperature 400 K (25). The nonequilibrium electrons distribute around the surface within the energy range of k_BT where k_B is the Boltzmann constant and T here is the system temperature without confusing to the time variant T in Eq. (3.8). Therefore the nonequilibrium electrons around the turning point 75 K is in the regime $\epsilon_F \gg k_BT \gg |\epsilon_k - \epsilon_F|$ where ϵ_F is the Fermi energy and ϵ_k is the electron energy with the momentum k. The e-e scattering time in this regime is estimated theoretically as (48)

$$\frac{1}{\tau_{ee}} = \frac{\pi\epsilon_F}{8\hbar}\left(\frac{k_BT}{\epsilon_F}\right)^2 \ln\frac{\epsilon_F}{k_BT}. \tag{3.18}$$

It is noted that the e-e scattering time in Eq. 3.18 is independent on the energy of the electrons and there is only one parameter, ϵ_F we need from the experimental data to estimate the e-e scattering time. In Fig. 3.2, we compare the momentum scattering time extracted from the experimental data in the supplementary material in the Ref. (25) and the theoretically estimate based on Eq. 3.18. They match very well when the temperature is above 30 K. The mismatch below 30 K maybe because the nonequilibrium electrons excited by the optical field is beyond the energy range of k_BT around the Fermi surface in the case of $T < 30$ K and Eq. 3.18 failed in this temperature regime. However, in a wide temperature regime, from 30 K to 150 K,

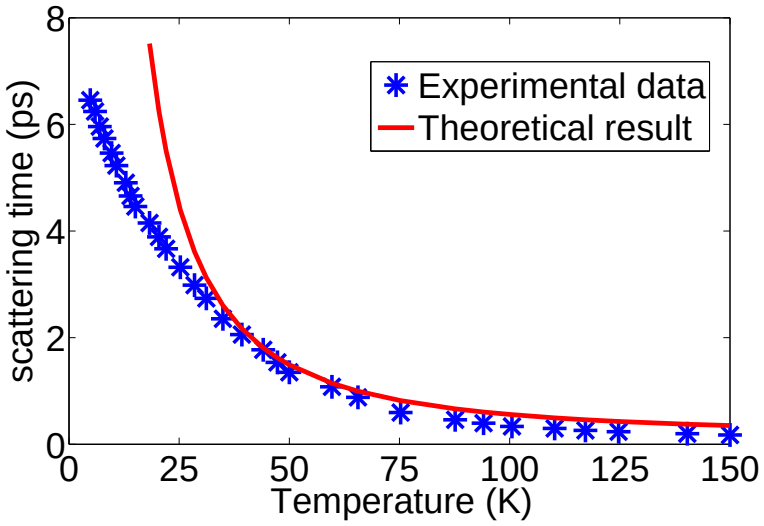

Fig. 3.2. τ_p vs T. The blue star is the momentum scattering time extracted from the figure of D_s vs T in the supplementary material in Ref (25) by using the relation $\tau = 2D_s/v_F^2$ where $v_F = \frac{\hbar k_F}{m^*}$ is the Fermi velocity and is estimated to be 4.32×10^5 m/s. The red line is the theoretical estimate based on the theory of the Ref. (48).

Fig. 3.2 indicates that the momentum scattering time felt by the spin relaxation is dominated by the e-e scattering time which is consistent to the spin Coulomb drag (49; 46) observed in the Ref. (24). Therefore, in the following discussion, we can safely neglect the impurity scattering in our theory.

3.2.2 Thermal average quantum kinetic equation

In the equilibrium state, the Keldysh Green's function satisfies (52)

$$\hat{G}_0^K(E,k) = (\hat{G}^R - \hat{G}^A)\tanh(\frac{E-\epsilon_F}{k_BT}). \tag{3.19}$$

When the quasiparticle approximation is valid, the Keldysh Green's function in the $E-\mathrm{k}$ space is still a peak even in the non-equilibrium state and has the form

$$\hat{G}^K(E,\mathrm{k};\mathrm{T},\mathrm{R}) = -2\pi\mathrm{i}\delta(\mathrm{E}-\epsilon_\mathrm{k})\hat{\mathrm{h}}, \tag{3.20}$$

where $\hat{h}(k,R,T)$ is the distribution function, defined as

$$\begin{aligned}\hat{h}_{\boldsymbol{k}}(\boldsymbol{R},T) &= -\int_{-\infty}^{\infty}\frac{dE}{2\pi i}\hat{G}^K_{\boldsymbol{k},E}(\boldsymbol{R},T) \\ &= g_c\sigma_0 + g_x\sigma_x + g_y\sigma_y + g_z\sigma_z.\end{aligned} \tag{3.21}$$

In the linear response limit, the non-equilibrium distribution function takes the form

$$\hat{h}_\mathrm{k}(R,T) = -\frac{f'(\epsilon_k)}{N_0}\hat{g}(\theta,R,T), \tag{3.22}$$

where N_0 is the density of state, θ is the angle between k and the x axis and

$$\hat{g} = \int N_0 d\epsilon_k \hat{h}_\mathrm{k}(R,T) \tag{3.23}$$

is the thermal average distribution function. We also introduce the density operator

$$\begin{aligned}
\hat{\rho}(E,R,T) &= i\int \frac{dE}{2\pi}\frac{d^2k}{(2\pi)^2}G^K_{k,E}(R,T) \\
&= \int \frac{d^2k}{(2\pi)^2}\hat{h}_{\rm k}({\rm R,T}) \\
&= \int \frac{d\theta}{2\pi}\int N_0\hat{h}_{\rm k}({\rm R,T}){\rm d}\epsilon_{\rm k} \\
&= \int \frac{d\theta}{2\pi}\hat{g}(-\int d\epsilon f'(\epsilon_k)) \\
&= \int \frac{d\theta}{2\pi}\hat{g}(\theta,{\rm R,T}). \qquad (3.24)
\end{aligned}$$

Multiply $-\int N_0 d\epsilon_k \int \frac{1}{2\pi i}dE$ on both sides of Eq.3.8, the left hand side takes the form

$$\partial_T\hat{g} + \boldsymbol{\nabla}_{\boldsymbol{R}}\cdot\{\frac{1}{2}\overline{\hat{\boldsymbol{V}}},\hat{g}\} + i[\overline{\boldsymbol{b}}\cdot\hat{\boldsymbol{\sigma}},\hat{g}] + \frac{\hat{g}}{\tau_{ee}}, \qquad (3.25)$$

where

$$\begin{aligned}
\overline{\hat{V}} &= \int -f'(\epsilon_k)\hat{V}({\rm k}){\rm d}\epsilon_{\rm k} = \hat{\rm V}(\overline{\rm k},\theta), \\
\overline{\boldsymbol{b}} &= \int -f'(\epsilon_k)\boldsymbol{b}(\boldsymbol{k}))d\epsilon_k = \overline{\boldsymbol{b}}(\overline{k},\overline{k^3},\theta), \qquad (3.26)
\end{aligned}$$

and the right hand side takes the form

$$\begin{aligned}
& -\int N_0 d\epsilon_k \frac{dE}{2\pi i}\underline{I}_{ee} = -\int N_0 d\epsilon_k \frac{dE}{2\pi i}\frac{dE'}{2\pi}\frac{d^2k'}{(2\pi)^2}\times \\
& \delta\underline{G}^K(D^R-D^A)(G^R-G^A) \\
& \times\left(\tanh(\frac{E}{2k_bT})+\coth(\frac{\omega}{2k_bT})\right) \\
= & -\int \frac{dE'}{2\pi}\frac{d^2k'}{(2\pi)^2}\delta\underline{G}^K \times \int \frac{dE}{2\pi}N_0 d\epsilon_k(D^R-D^A) \\
& \times(G^R-G^A)\left(\tanh(\frac{E}{2k_bT})+\coth(\frac{\omega}{2k_bT})\right) \\
\approx & \ \hat{\rho}(R,T)\times\frac{1}{\tau_{ee}}. \qquad (3.27)
\end{aligned}$$

Therefore, the kinetic equation in Eq. 3.8 is converted to the equation of the thermal average distribution $\hat{g}(\theta, \boldsymbol{R}, T)$ and the density function $\hat{\rho}(\mathrm{R}, \mathrm{T})$ which takes the form

$$\partial_T \hat{g} + \boldsymbol{\nabla}_{\boldsymbol{R}} \cdot \{\frac{1}{2}\overline{\hat{\boldsymbol{V}}}, \hat{g}\} + i[\overline{\boldsymbol{b}} \cdot \hat{\boldsymbol{\sigma}}, \hat{g}] + \frac{\hat{g}}{\tau_{ee}} = \frac{\hat{\rho}(\boldsymbol{R}, T)}{\tau_{ee}} \tag{3.28}$$

Eq. 3.28 gives the kinetic equation of the thermal average distribution function $\hat{g}$ and the density matrix $\hat{\rho}(\mathrm{R}, \mathrm{T})$. However, the spin-charge dynamic equation normally is the equation of the density $\hat{\rho}$. Therefore it is the key process to get rid of the distribution equation from the kinetic equation, Eq. 3.28, and convert it to an equation only containing $\hat{\rho}$. This is not easily to be done in the presence of SOIs. E. G. Mishchenko *et al.* (31) treated the gradient term $\nabla\hat{G}^K$, as a perturbation and developed a self consistent method to derive the diffusion equation to the any order of the $\nabla\hat{g}$ in principle. However this method is restricted to the Rashba SOI and becomes harder when calculating the higher order gradient terms or considering the linear and cubic Dresselhaus SOC. B. A. Bernevig *et al.* (44) point out that in the balistic regime $ql > 1$, where q is the spin-charge wave length and l is the mean free path, we have to consider the higher order gradient terms $\nabla\hat{G}^K$. This means in the ballistic regime, the spin-charge dynamic equation is not dominated by the second order of the spacial differential operators ∇^2 but need to consider the infinite summation over the gradient expansion. However, B. A. Bernevig *et al.* (44) only did it in the very special case when $\alpha = \beta_1$ and $\beta_3 = 0$. For a generic SOI, it is almost impossible to finish the infinite summation. Therefore in this work, we abandon the idea of the gradient expansion of $\nabla\hat{G}^K$ and provide a different way to obtain the spin-charge dynamic equation for the general SOIs.

3.2.3 Spin-charge density dynamic equation-valid in the both weak and strong SOC regime

The thermal average distribution function and density matrix can be generally written as

$$\begin{aligned}\hat{g} &= g_c\sigma_0 + g_x\sigma_x + g_y\sigma_y + g_z\sigma_z \\ \hat{\rho} &= \rho_c\sigma_0 + \rho_x\sigma_x + \rho_y\sigma_y + \rho_z\sigma_z.\end{aligned} \tag{3.29}$$

The third term on the left hand side of Eq. 3.28 has the form

$$[\overline{b}x\sigma_x + \overline{b}_y\sigma_y, \hat{g}] = 2i\left((\overline{b}_x g_y - \overline{b}_y g_x)\sigma_z - \overline{b}_x g_z\sigma_y + \overline{b}_y g_z\sigma_x\right). \tag{3.30}$$

which couples different spin components and generates spin precession. The second term on the left hand side of Eq. 3.28 contains the SOC velocity operators $\hat{v}_{so} = \partial H_{so}/\partial_k$ which gives

$$\begin{aligned}& \{\lambda_1\sigma_y\partial_x + \lambda_2\sigma_x\partial_y, \hat{g}\} \\ = \;& (\lambda_1\partial_x g_y + \lambda_2\partial_y g_x)\sigma_0 + \lambda_1\partial_x g_c\sigma_y + \lambda_2\partial_y g_c\sigma_x,\end{aligned} \tag{3.31}$$

which couples charge and spin by the finite $\boldsymbol{\nabla}\hat{g}$ which indicates non-uniform charge or spin distribution in the real space. The other terms of Eq. 3.30 do not couple spin or charge components. If we multiply σ_i where $i = 0, x, y, z$ and calculate the trace, using the fact that $\mathrm{Tr}(\sigma_\mathrm{i}\sigma_\mathrm{j})/2 = \delta_\mathrm{ij}$, Eq. 3.28 can be rewritten as

$$\begin{aligned}\left((\partial_T + \frac{1}{\tau} + \frac{\overline{\boldsymbol{k}}}{m}\cdot\boldsymbol{\nabla})g_c + \lambda_1\partial_x g_y + \lambda_2\partial_y g_x\right)\sigma_0 &= \frac{\rho_c}{\tau}\sigma_0 \\ \left((\partial_T + \frac{1}{\tau} + \frac{\overline{\boldsymbol{k}}}{m}\cdot\boldsymbol{\nabla})g_x + \lambda_2\partial_y g_c + 2i\overline{b}_y g_z\right)\sigma_x &= \frac{\rho_x}{\tau}\sigma_x\end{aligned}$$

$$\left((\partial_T + \frac{1}{\tau} + \frac{\overline{\boldsymbol{k}}}{m}\cdot\boldsymbol{\nabla})g_y + \lambda_1\partial_x g_c - 2i\overline{b}_x g_z\right)\sigma_y = \frac{\rho_y}{\tau}\sigma_y$$
$$\left((\partial_T + \frac{1}{\tau} + \frac{\overline{\boldsymbol{k}}}{m}\cdot\boldsymbol{\nabla})g_z + 2i(\overline{b}_x g_y - \overline{b}_y g_x)\right)\sigma_z = \frac{\rho_z}{\tau}\sigma_z \tag{3.32}$$

where $\overline{\boldsymbol{k}}$ is the thermal average of the momentum. Above we have multiplied again by the corresponding matrix to remind ourselves of which component belongs to which. Hence, we can obtain the 4×4 kinetic equation of the coefficients $g_{c(x,y,z)}$ and $\rho_{c(x,y,z)}$ which takes the form

$$\hat{K}\begin{pmatrix} g_c \\ g_x \\ g_y \\ g_z \end{pmatrix} = \begin{pmatrix} \rho_c \\ \rho_x \\ \rho_y \\ \rho_z \end{pmatrix}, \tag{3.33}$$

where

$$\hat{K} = \begin{pmatrix} \tilde{\Omega} & -i\lambda_2 q_y\tau & i\lambda_1 q_x\tau & 0 \\ -i\lambda_2 q_y\tau & \tilde{\Omega} & 0 & -2\overline{b}_y\tau \\ i\lambda_1 q_x\tau & 0 & \tilde{\Omega} & 2\overline{b}_x\tau \\ 0 & 2\overline{b}_y\tau & -2\overline{b}_x\tau & \tilde{\Omega} \end{pmatrix} \tag{3.34}$$

where $\tilde{\Omega} = 1 - i\omega\tau + \boldsymbol{q}\cdot\boldsymbol{v}\tau$ and θ is angle between $\boldsymbol{k}$ and x axis. Here we have Fourier transformed ∂_T and $\partial_{x(y)}$ to $-i\omega$ and $iq_{x(y)}$ which are the frequency and wavelength of the spin polarization wave in the experiments. To further obtain the spin dynamic equation, we simply multiply $\hat{K}^{-1}$ on both sides of Eq. 3.28 and integrate out the angle θ. The inverse of $\hat{K}$ is easy to be obtained for the generic SOIs because it is just the inverse of a 4×4 matrix. Therefore we provide a way to derive the spin dynamic equation in the presence of the general SOIs.

Before our further discussion of the spin dynamic equation, we would like to emphasize the two advantages of our method. First, the inverse of the matrix $\hat{K}$ is equivalent to the infinite summation of the gradient expansion but much easier to be calculated exactly. In the Sec. 3.4, it is shown that in the case of $\alpha = \beta_1$ and $\beta_3 = 0$, we obtain the same spin dynamics modes to those obtained by the infinite summation of the gradient expansion of $\nabla\hat{G}^K$ (44). Second, we need not to guess the form of the nonequilibrium distribution function $\hat{g}$ before we obtain the spin dynamics equation. The nonequilibrium distribution function is often be expanded on spherical harmonics (Eq.(7.79) in the Ref.(52)) before we solve the kinetic equation. Normally in the system without SOIs, it is enough to stop the expansion on the degree 1 of the spherical harmonics. However, in the presence of the SOIs, especially considering the cubic Dresselhaus SOI, the distribution function may contain the spherical harmonics up to the degree 3. Therefore it is very difficult and complicated to guess the correct form of the nonequilibrium distribution function by expand it on the right degree of spherical harmonics. Our method does not have this difficulty and is equivalent to consider all possible spherical harmonics in the nonequilibrium distribution function.

To simplify our discussion of the spin dynamic equation, we consider the spin wave vector only along x direction and take $q_y = 0$. Because $q \ll k_F$, the spin-charge coupling term $i\lambda_{1(2)}q_{x(y)}\tau$ is much smaller than spin-spin coupling term $i\lambda_{1(2)}k\tau$ in Eq. 3.34 and we neglect the spin-charge coupling and only focus on the spin space of Eq. 3.34 In this case, using the definition Eq. 3.24 the spin-charge dynamic equation of the density coefficient $\rho_{c(x,y,z)}$ can be obtained as

$$\int \frac{d\theta}{2\pi} \begin{pmatrix} g_x \\ g_y \\ g_z \end{pmatrix} = \begin{pmatrix} \rho_x \\ \rho_y \\ \rho_z \end{pmatrix} = \hat{D} \begin{pmatrix} \rho_x \\ \rho_y \\ \rho_z \end{pmatrix}, \tag{3.35}$$

where $\hat{D} = \int \frac{d\theta}{2\pi} \hat{K}_s^{-1}$ and $\hat{K}_s^{-1}$ takes the form

$$\hat{K}_s^{-1} = \frac{\begin{pmatrix} \tilde{\Omega}^2 + 4\overline{b}_x^2\tau^2 & 4\overline{b}_x\overline{b}_y\tau^2 & 2\overline{b}_y\tau\tilde{\Omega} \\ 4\overline{b}_x\overline{b}_y\tau^2 & \tilde{\Omega}^2 + 4\overline{b}_y^2\tau^2 & -2\overline{b}_x\tau\tilde{\Omega} \\ -2\overline{b}_y\tau\tilde{\Omega} & 2\overline{b}_x\tau\tilde{\Omega} & \tilde{\Omega}^2 \end{pmatrix}}{\tilde{\Omega}^3 + 4\overline{b}^2\tau^2\tilde{\Omega}}. \tag{3.36}$$

Eq.3.35 is the spin dynamics equation in the frequency-momentum space.

3.3 Spin dynamics in the weak SOC regime

In this section, we focus on the spin dynamics in the weak SOC regime which is normally at relative high temperature, say above 35K (25).

3.3.1 Only DP spin relaxation mechanism

In the regime where $\lambda_{1(2)}k\tau \ll 1$, $ql \ll 1$, which is called the weak SOC regime, the spin-charge dynamic equation can be written as

$$(-i\tilde{\omega} + \frac{1}{2}(\tilde{q}_x^2 + \tilde{q}_y^2)) \begin{pmatrix} \rho_x \\ \rho_y \\ \rho_z \end{pmatrix} + \hat{D}_{so} \begin{pmatrix} \rho_x \\ \rho_y \\ \rho_z \end{pmatrix} = 0 \tag{3.37}$$

where

$$\hat{D}_{so} = \begin{pmatrix} \tilde{\Omega}_{so}^2(\frac{1}{2} + \tilde{\alpha}\tilde{\beta}) & 0 & i(\tilde{\alpha} + \tilde{\beta})\tilde{\Omega}_{so}\tilde{q}_x \\ 0 & \tilde{\Omega}_{so}^2(\frac{1}{2} - \tilde{\alpha}\tilde{\beta}) & i(\tilde{\alpha} - \tilde{\beta})\tilde{\Omega}_{so}\tilde{q}_y \\ -i(\tilde{\alpha} + \tilde{\beta})\tilde{\Omega}_{so}\tilde{q}_x & -i(\tilde{\alpha} - \tilde{\beta})\tilde{\Omega}_{so}\tilde{q}_y & \tilde{\Omega}_{so}^2 \end{pmatrix}$$

$$\tilde{\alpha} = \frac{\alpha}{\sqrt{\alpha^2 + (\beta_1 - \beta_3)^2 + \beta_3^2}}$$

$$\tilde{\beta} = \frac{\beta_1 - \beta_3}{\sqrt{\alpha^2 + (\beta_1 - \beta_3)^2 + \beta_3^2}}, \tag{3.38}$$

$\tilde{\Omega}_{so} = \Omega_{so}\tau$ and $\Omega_{so} = 2\sqrt{\alpha^2 + (\beta_1 - \beta_3)^2 + \beta_3^2}k_F$ is the spin precession frequency due to the SOC. The first term on the left hand side of Eq. 3.37 is the normal diffusion equation without SOIs. The second term is corresponding to the average torque exerted by the SOC in the momentum space which gives the correction of diffusion equation due to the generic SOIs. The detailed calculation of the elements of the matrix $\hat{D}$ is shown in appendix B.3.

Our spin diffusion equation, Eq. 3.37, is equivalent to the spin diffusion equation in Ref. (33) at zero temperature where $k = k_F$. However only considering D-P mechanism seems not to be enough to explain the temperature dependence of the enhanced-lifetime of the spin helix mode (25), which first increased with increasing temperature from 5 K to 75 K and then decreased with further increasing temperature. Because the density of states is a constant for the 2DEG, the chemical potential shift at finite temperature is of the order of $(\frac{kT}{E_F})^4 = 0.0039$ when $T = 100$ K according to the Sommerfeld expansion. Our numerical calculation gives $E_{\rm f} = 398.15$ K at $T = 100$ K which is consistent to the analytical prediction. If assuming that $\chi(E) = -f'(E)$, at $T = 100$ K we have

$$\begin{aligned} \overline{k} &= \int dE - f'(E)k = 0.98k_F \\ \overline{k^3} &= \int dE - f'(E)k^3 = 1.1k_F^3. \end{aligned} \tag{3.39}$$

which prove that the thermal average $\overline{k}$ and $\overline{k^3}$ are not changed too much from $0K$ to 100 K. Therefore the increasing of the thermal average cubic Dresselhaus SOI was not sufficiently strong to account for the non-monotonic T-dependence of the enhanced-lifetime of the SHM. Another evidence for this statement is from the Fig. 3c in Ref. (25). The mobility is reduced to avoid the ballistic crossover and the spin life time is measured in five different temperatures as a function of spin polarized wave

vector q. It is found that at $q = 1.26 \times 10^4$ cm^{-1} which is close to the SU(2) points, the spin life time is the maximum at the lowest temperature 5 K and minimum at the highest temperature 250 K. When q is away from the SU(2) point such as $q = 0$ or $q = 2.5 \times 10^4$ cm^{-1}, the spin life time is the minimum at the lowest temperature 5 K and maximum at the highest temperature 250 K. As a result, when q is far away from the SU(2) point, the enhanced-lifetime of spin helix mode matches the description of D-P mechanism that the spin life time is inversely proportional to the momentum scattering time. When q is close to the SU(2) point, the turning point, at which the spin life time changes from increasing to decreasing with increasing the temperature, is lower than 5 K. The turning point at so low temperature can not be the consequence of the thermal average of the cubic Dresselhaus SOI (25).

3.3.2 EY mechanism in the 2DEG with the e-e interaction

Because D-P mechanism is not sufficient to account for the T-dependence of the SHM life time, we have to consider the E-Y mechanism which is proportional to the momentum scattering time and opposite to the case of D-P mechanism. There are two processes involved: that of Elliott (55) and that of Yafet (56). In the Elliott process, the scattering potential is spin independent. The spin flip is due to the SOC on the Bloch state, say the admixture of the Pauli up and down spins through the coupling between the conduction and valence bands. Therefore, the Elliott mechanism has the same origin of the Rashba SOI in the conduction band which is also from the coupling between conduction and valence bands. In the Yafet process spin flips are directly from the scattering potential with the well known form $\frac{\hbar}{4m_0c^2}(\boldsymbol{\nabla} V \times \boldsymbol{P}) \cdot \boldsymbol{\sigma}$ so that the potential alone couples opposite spins. In the GaAs/AlGaAs 2DEG, it is shown in appendix B.1 the Elliott mechanism is much larger than the Yafet mechanism. As a result, in the following discussion, we only consider the Elliott processes. The Elliott mechanism can be derived from the unitary transformation matrix based

on the Löwdin partitioning (54). The coordinate $\boldsymbol{r}$ after unitary transformation takes the form (57)

$$\begin{aligned}\boldsymbol{r}_{eff} &= \boldsymbol{r} - \frac{P^2}{3}(\frac{1}{E_0^2} - \frac{1}{(E_0+\Delta_0)^2})\boldsymbol{k}\times\boldsymbol{\sigma} = \boldsymbol{r} - \gamma\boldsymbol{k}\times\boldsymbol{\sigma}, \\ \gamma &= \frac{P^2}{3}(\frac{1}{E_0^2} - \frac{1}{(E_0+\Delta_0)^2})\boldsymbol{k}\times\boldsymbol{\sigma}\end{aligned} \tag{3.40}$$

where $P = \frac{i\hbar^2}{m_0} < S|\nabla|R >$, $|S\rangle$ is the s-wave like local orbital state, $R = X, Y, Z$ are the p-wave like local orbital states, E_0 is the band gap between Γ_6^- conduction band and Γ_8^+ valence band and Δ_0 is the SOC gap between the bands of Γ_7^+ and Γ_8^+ (54). Any coordinates dependent potential will be modified by the second term in Eq. 3.40. For example, the impurity scattering potential has the form

$$V_{imp}(\boldsymbol{r}_{eff}) = V_{imp}(\boldsymbol{r}) - \gamma(\boldsymbol{\nabla}_{\boldsymbol{r}}V_{imp}(\boldsymbol{r})\times\boldsymbol{k})\cdot\boldsymbol{\sigma} \tag{3.41}$$

and the Coulomb interaction now has the form

$$\begin{aligned}V_{e-e}(\boldsymbol{r}_{1eff}, \boldsymbol{r}_{2eff}) &= V_{e-e}(\boldsymbol{r_1}, \boldsymbol{r_2}) - \gamma(\boldsymbol{\nabla}_{\boldsymbol{r_1}}V_{e-e}\times\boldsymbol{k}_1)\cdot\boldsymbol{\sigma} \\ &\quad -\gamma(\boldsymbol{\nabla}_{\boldsymbol{r_2}}V_{e-e}\times\boldsymbol{k}_2)\cdot\boldsymbol{\sigma},\end{aligned} \tag{3.42}$$

where the subscripts 1 and 2 of the space coordinates represent the two interacting electrons respectively. Therefore the spin-orbit coupled scattering potential has the form

$$\hat{V}_{so}(\boldsymbol{r}) = -\gamma(\boldsymbol{\nabla}_{\boldsymbol{r}}V(\boldsymbol{r})\times\boldsymbol{k})\cdot\boldsymbol{\sigma}, \tag{3.43}$$

where $V(\boldsymbol{r}) = (V_{imp} + V_{e-e})$ is the spin independent momentum scattering potential. The spin relaxation rate due to the E-Y mechanism in the 3D bulk material has the form (58)

$$\frac{1}{\tau_{EY}(\epsilon_k)} = A\left(\frac{\Delta_0}{E_0+\Delta_0}\right)^2\left(\frac{\epsilon_k}{E_0}\right)^2\frac{1}{\tau(\epsilon_k)}, \tag{3.44}$$

where the numerical factor A is of the order of 1 and dependent on the scattering mechanism (58) such as e-e interaction (59) and $\tau(\epsilon_k)$ is the momentum scattering time at energy ϵ_k. Because the non-equilibrium electrons distribute around the Fermi surface within the energy range k_BT, the e-e scattering time is independent on the energy ϵ_k according to Eq. 3.18 and is notated as τ. In the 2DEG, the momentum k_z is quantized. In this case, altough and the average of $\langle k_z\rangle = 0$, $\langle k_z^2\rangle \approx (\frac{\pi}{d})^2$ which gives the linear Dresselhaus SOI (25). For the same reason, when considering E-Y mechanism, we also assume $\langle k_z^2\rangle \approx (\frac{\pi}{d})^2$ where d is the width of the quantum well. Therefore, the E-Y mechanism in the 2DEG can be written as

$$\begin{aligned}\frac{1}{\tau_{EY,x}} = \frac{1}{\tau_{EY,y}} &= A(1+\frac{2\langle k_z^2\rangle}{k_F^2})\left(\frac{\Delta_0}{E_0+\Delta_0}\right)^2\left(\frac{\epsilon_k}{E_0}\right)^2\frac{1}{\tau},\\ \frac{1}{\tau_{EY,z}} &= A\frac{4\langle k_z^2\rangle}{k_F^2}\left(\frac{\Delta_0}{E_0+\Delta_0}\right)^2\left(\frac{\epsilon_k}{E_0}\right)^2\frac{1}{\tau},\end{aligned} \tag{3.45}$$

where $\tau_{\mathrm{EY,x(y,z)}}$ are the spin relaxation time for the spin polarization along x, y, z direction respectively due to the E-Y mechanism. Appendix B.1 gives the detailed derivation of the E-Y mechanism.

3.3.3 Temperature dependence of the spin relaxation modes

In this sub-section, we will show that the temperature dependence of the spin relaxation modes, especially the enhanced-lifetime of the SHM, is the consequence of the competition between the D-P and E-Y mechanisms. By adding the E-Y

mechanism on the Eq. 3.37, the spin-charge dynamics containing both D-P and E-Y mechanism takes the form

$$
\begin{aligned}
&(-i\tilde{\omega}+\frac{1}{2}(\tilde{q}_x^2+\tilde{q}_y^2))\begin{pmatrix} n_x \\ n_y \\ n_z \end{pmatrix}+ \\
&\begin{pmatrix} \tilde{\Omega}_{so}^2(\frac{1}{2}+\tilde{\alpha}\tilde{\beta})+\kappa_1 & 0 & i(\tilde{\alpha}+\tilde{\beta})\tilde{\Omega}_{so}\tilde{q}_x \\ 0 & \tilde{\Omega}_{so}^2(\frac{1}{2}-\tilde{\alpha}\tilde{\beta})+\kappa_1 & i(\tilde{\alpha}-\tilde{\beta})\tilde{\Omega}_{so}\tilde{q}_y \\ -i(\tilde{\alpha}+\tilde{\beta})\tilde{\Omega}_{so}\tilde{q}_x & -i(\tilde{\alpha}-\tilde{\beta})\tilde{\Omega}_{so}\tilde{q}_y & \tilde{\Omega}_{so}^2+\kappa_1^{\perp} \end{pmatrix}\begin{pmatrix} n_x \\ n_y \\ n_z \end{pmatrix} \\
=\ & 0. \qquad (3.46)
\end{aligned}
$$

where

$$
\begin{aligned}
\kappa_1 &= A(1+\frac{2\langle k_z^2\rangle}{k_F^2})\left(\frac{\Delta_0}{E_0+\Delta_0}\right)^2\left(\frac{\epsilon_k}{E_0}\right)^2, \\
\kappa_1^{\perp} &= A\frac{4\langle k_z^2\rangle}{k_F^2}\left(\frac{\Delta_0}{E_0+\Delta_0}\right)^2\left(\frac{\epsilon_k}{E_0}\right)^2, \qquad (3.47)
\end{aligned}
$$

Here, according to Eq. 3.39, we take the thermal average of the momentum $\overline{k}=k_F$. To simplify our discussion, we assume that the spin polarization is uniform in y direction and non-uniform in x direction with finite $\tilde{q}_x$. In this case the spin polarization along y direction is not coupled to other two components of spin polarization. Based on the Eq. 3.46, the eigen mode of the spin polarization along y direction, has the form

$$
i\tilde{\omega}_y = \frac{1}{2}\tilde{q}_x^2+\tilde{\Omega}_{so}^2(\frac{1}{2}-\tilde{\alpha}\tilde{\beta})+\kappa_1, \qquad (3.48)
$$

where $\tilde{\omega}_y$ is the normalized eigen frequency of spin polarization along y direction. At the $SU(2)$ symmetric point (47) where $\alpha=\beta_1$ and $\beta_3=0$, $(1/2-\tilde{\alpha}\tilde{\beta})=0$ and the effect of the D-P mechanism on the spin polarization along y direction is zero. This

is consistent to the fact that the effective magnetic field due to SOC in this case is always along y direction.

Next we focus on the other two spin dynamic modes which have the form

$$\begin{aligned} i\tilde{\omega}_{\pm} &= \kappa_1^s + \frac{1}{2}\tilde{q}_x^2 + \tilde{\Omega}_{so}^2(\frac{3}{4} + \frac{\tilde{\alpha}\tilde{\beta}}{2}) \\ &\quad \pm\sqrt{\left(\tilde{\Omega}_{so}^2(\frac{\tilde{\alpha}\tilde{\beta}}{2} - \frac{1}{4}) + \kappa_1^a\right)^2 + (\tilde{\alpha}+\tilde{\beta})^2\tilde{\Omega}_{so}^2\tilde{q}_x^2}, \\ \kappa_1^s &= \frac{\kappa_1 + \kappa_1^{\perp}}{2} \quad \text{and} \quad \kappa_1^{\mathrm{a}} = \frac{\kappa_1 - \kappa_1^{\perp}}{2} \end{aligned} \tag{3.49}$$

where $\tilde{\omega}_{\pm}$ are the normalized eigen frequencies of the reduced- and enhanced-lifetime of the two SHMs (25) respectively. The maximum enhanced-lifetime of the spin helix mode happens when $\alpha = \beta_1$, $\beta_3 = 0$ and $q = 4m_{eff}\alpha = Q$. In this case, we have $\tilde{\alpha} = \tilde{\beta} = \alpha/\sqrt{\alpha^2 + \beta_1^2} = \frac{\sqrt{2}}{2}$ and $\tilde{q} = 4m_{eff}\alpha v_f\tau = \sqrt{2}\Omega_{so}\tau = \sqrt{2}\tilde{\Omega}_{so}$. However, in the material such as GaAs, the cubic Dresselhaus SOI is the consequence of bulk inversion asymmetry (BIA) and is inevitable. When considering the cubic Dresselhaus SOI, the maximus spin life time is observed at $\beta_1 - \beta_3 = \alpha$ (25) which is consistent to the theoretical prediction (33) at zero temperature. When $\beta_3 \ll \alpha$, the maximum enhanced-lifetime of the SHM is still at $Q = 4m_{eff}\alpha$ shown in Fig. 3.3. As a result, the Rashba SOC strength can be detected by the relation $\alpha = Q/4m_{eff}$ which gives the relation

$$\begin{aligned} \Omega_{so} &= 2\sqrt{\alpha^2 + (\beta_1 - \beta_3)^2 + \beta_3^2}k_F \\ &\approx 2\sqrt{2}\alpha k_F = \frac{Qk_F}{\sqrt{2}m_{eff}}. \end{aligned} \tag{3.50}$$

Taking $q_x = 4m_{eff}\alpha$ and substituting the above relation to Eq. 3.48, we obtain the reduced- and enhanced-lifetime of the spin helix modes as

$$i\omega_{\pm} = \frac{\kappa_1^s}{\tau} + \kappa_2^{\pm}\tau, \tag{3.51}$$

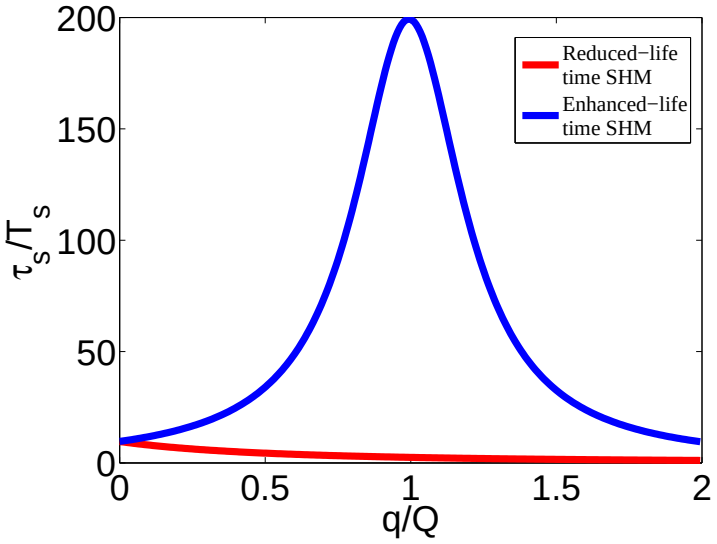

Fig. 3.3. The reduced-lifetime and enhanced-lifetime of the SHMs. The x axis is the spin wave vector normalized by $Q = 4m_{eff}\alpha$ and the y axis is the spin life time normalized by the spin precession period $T_s = \frac{2\pi}{\Omega_{so}}$. $\Omega_{so}\tau = 0.1$ is taken to satisfy the weak SOC condition and $\beta_3/\beta_1 = 0.16$ from the experimental data (25). The maximal enhanced-lifetime is still very close to Q although the cubic Dresselhaus SOI is nonzero.

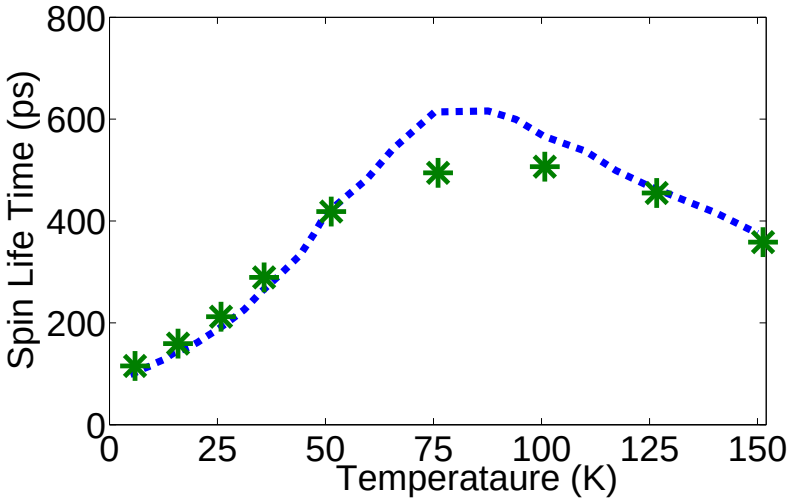

Fig. 3.4. The green stars are the enhanced life time of the spin helix modes extracted from the Ref. (25). The blue dash line is our theoretical result by substituting τ in Fig. 3.2 to our spin dynamic equation.

$$\kappa_2^{\pm} = \Omega_{so}^2 \left(\frac{7}{4} + \frac{\tilde{\alpha}^2}{2} \pm \sqrt{\left((\frac{\tilde{\alpha}^2}{2} - \frac{1}{4}) + \frac{\kappa_1^a}{\tilde{\Omega}_{so}^2} \right)^2 + 8 \times \tilde{\alpha}^2} \right). \tag{3.52}$$

where $\pm$ is corresponding to the reduced- and enhanced-lifetime of the SHMs respectively.

We first plot the enhanced-lifetime of the spin helix mode in Fig. 3.4 and show its consistence to the experimental results in the Ref.(25). The system we are considering is the GaAs/AlGaAs quantum well in the Ref. (25). Its width is 11nm which gives $\beta_3/\beta_1 = \langle k_F^2 \rangle / 4\langle k_z^2 \rangle = 0.16$ (25). Therefore, in this system, $\beta_1 - \beta_3 = \alpha \gg \beta_3$ and Ω_{so} is estimated to be 0.356 THz based on the Eq. 3.50. The band gap $E_0 = 1.519$ eV, $\Delta_0 = 0.341$ eV. To fit the experimental data, Fig. 3.4, the only fitting parameter we choose is $A = 4.0$ which is the order of 1 and consistent to the estimate in the Ref.(58).

Based on the Eq. 3.51, both the reduced- and the enhanced-lifetime of the SHMs exist the maximal spin life time as a result of the competition between the D-P and E-Y mechanism. The critical momentum scattering times $\tau_c^{\pm}$ when the spin life time reach its maximum take the value

$$\tau_c^+ = \sqrt{\frac{\kappa_1^s}{\kappa_+}} = 0.029\text{ps},$$
$$\tau_c^- = \sqrt{\frac{\kappa_1^s}{\kappa_-}} = 0.51\text{ps}. \tag{3.53}$$

This is the result of the competition of E-Y and D-P mechanisms. It is noted that $\tau_+ \ll \tau_-$ which indicates the reduced-lifetime needs much higher temperature than the enhanced-lifetime to reach its maximum. Actually $\tau_c^+ = 0.029$ ps is smaller than the minimum momentum scattering time 0.04 ps estimated from the spin life time of the enhanced SHM is 100 ps at $T = 300$ K based on the Eq. 3.52. This is the why the reduced-lifetime of the SHM increase monotonically with increasing T.

3.4 Spin relaxation in the strong SOC regime

In this appendix, we show that our theory can reproduce the theoretical results of the spin relaxation in the case of $\alpha = \beta_1$, $\beta_3 = 0$ (44) and in the case of only Rashba or linear Dresselhaus SOI (51) in the strong SOC regime at zero temperature.

3.4.1 $\alpha = \beta_1$

The persistent SHM is discovered in the case of $\alpha = \beta_1$, $\beta_3 = 0$ and q is along x direction. In this case, the elements of the matrix $\hat{D}$, corresponding to the reduced-

and enhanced-lifetime of the SHMs, in the spin-charge dynamic equation 3.35 take the form

$$\begin{aligned} D_{11} &= D_{33} = \frac{1}{2\sqrt{(1-i\tilde{\omega})^2+(\tilde{q}_x+\tilde{\Omega}_{so})^2}} \\ &+ \frac{1}{2\sqrt{(1-i\tilde{\omega})^2+(\tilde{q}_x-\tilde{\Omega}_{so})^2}} \\ D_{13} &= -D_{31} = \frac{i}{2\sqrt{(1-i\tilde{\omega})^2+(\tilde{q}_x+\tilde{\Omega}_{so})^2}} \\ &- \frac{i}{2\sqrt{(1-i\tilde{\omega})^2+(\tilde{q}_x-\tilde{\Omega}_{so})^2}} \end{aligned} \tag{3.54}$$

where $\Omega_{so} = 2\lambda_1 k_F \tau$. The eigenmodes satisfy the equation

$$\begin{aligned} (1-D_{11})^2 + D_{13}^2 = & \frac{\left(-1+\sqrt{(1-i\tilde{\omega})^2+\left(\tilde{q}_x-\tilde{\Omega}_{so}\right)^2}\right)}{\sqrt{(1-i\tilde{\omega})^2+\left(\tilde{q}_x-\tilde{\Omega}_{so}\right)^2}} \\ & \times \frac{\left(-1+\sqrt{(1-i\tilde{\omega})^2+\left(\tilde{q}_x+\tilde{\Omega}_{so}\right)^2}\right)}{\sqrt{(1-i\tilde{\omega})^2+\left(\tilde{q}_x+\tilde{\Omega}_{so}\right)^2}} = 0 \end{aligned} \tag{3.55}$$

which gives the spin relaxation eigenmodes as

$$i\tilde{\omega} = 1 \pm \sqrt{1-(\tilde{q}_x \pm \tilde{\Omega}_{so})^2}, \tag{3.56}$$

and is consistent to the result in Ref. (44).

3.4.2 Only Rashba or linear Dresselhaus SOI

In the presence of the Rashba or linear Dresselhaus SOI, we only discuss spin relaxation of the uniform spin polarization because as far as we know there does not exist the analytical form of the spin relaxation eigenmodes for the non-uniform spin

polarization in the presence of only the Rashba or linear Dresselhaus SOI. For the uniform spin polarization, the off diagonal elements of the dynamic matrix $\hat{D}$ in the Eq. 3.35 is zero because the angle average of the effective magnetic field $\boldsymbol{b}$ is zero. Therefore we only need to focus on the diagonal terms which have the form

$$\begin{aligned} D_{11} = D_{22} &= \frac{\tilde{\Omega}^2 + \tilde{\Omega}_{so}^2/2}{\tilde{\Omega}(\tilde{\Omega}^2 + \tilde{\Omega}_{so}^2)}, \\ D_{33} &= \frac{\tilde{\Omega}}{\tilde{\Omega}^2 + \tilde{\Omega}_{so}^2}. \end{aligned} \tag{3.57}$$

The spin relaxation mode of the spin polarization along z direction satisfies the equation $1 - D_{33} = 0$ and is solved to has the form

$$i\tilde{\omega}_z = \frac{1}{2}\left(1 - \sqrt{1 - 4\tilde{\Omega}_{so}^2}\right), \tag{3.58}$$

which is identical to our previous theoretical result (51) at zero temperature limit which has been shown to consistent to the experimental observation (36).

3.5 Conclusion

We have developed a consistent microscopic approach to explore the spin dynamics in the presence of SOC, impurity scattering and e-e interaction at finite temperature. The e-e interactions are involved by using the Keldysh Green's function. Because the D-P mechanism is suppressed for the SOC enhanced SHM, the E-Y mechanism is dominated in the high temperature for this mode. By choosing the reasonable parameter of E-Y mechanism, we show that our theory of enhanced-lifetime of the spin helix mode matches the experimental data quantitatively. Our theory is also shown to be able to recover the several previous theoretical results, which are only valid in the non-interacting system.

REFERENCES

[1] I. Genish, Y. Kats, L. Klein, J. W. Reiner, and M. R. Beasley, Journal of Applied Physics **95**, 6681 (2004).

[2] P. Wisniewski, Applied Physics Letters **90**, 192106 (2007).

[3] S. Datta and B. Das, Applied Physics Letters **56**, 665 (1990).

[4] J. M. Kikkawa and D. D. Awschalom, Phys. Rev. Lett. **80**, 4313 (1998).

[5] B. T. Jonker et al., Phys. Rev. B **62**, 8180 (2000).

[6] A. T. Hanbicki, B. T. Jonker, G. Itskos, G. Kioseoglou, and A. Petrou, Applied Physics Letters **80**, 1240 (2002).

[7] X. Jiang et al., Phys. Rev. Lett. **90**, 256603 (2003).

[8] X. Lou et al., Nature Physics **3**, 197 (2007).

[9] I. Appelbaum, B. Huang, and D. J. Monsma, Nature **447**, 295 (2007).

[10] J. E. Hirsch, Phys. Rev. Lett. **83**, 1834 (1999).

[11] S. Murakami, N. Nagaosa, and S.-C. Zhang, Science **301**, 1348 (2003).

[12] J. Sinova et al., Phys. Rev. Lett. **92**, 126603 (2004).

[13] Y. K. Kato, R. C. Myers, A. C. Gossard, and D. D. Awschalom, Science **306**, 1910 (2004).

[14] J. Wunderlich, B. Kaestner, J. Sinova, and T. Jungwirth, Phys. Rev. Lett. **94**, 047204 (2005).

[15] C. L. Kane and E. J. Mele, Phys. Rev. Lett. **95**, 226801 (2005).

[16] C. L. Kane and E. J. Mele, Phys. Rev. Lett. **95**, 146802 (2005).

[17] B. Bernevig and S. Zhang, Phys. Rev. Lett. **96** (2006).

[18] B. A. Bernevig, T. L. Hughes, and S.-C. Zhang, Science **314**, 1757 (2006).

[19] L. Fu, C. L. Kane, and E. J. Mele, Phys. Rev. Lett. **98** (2007).

[20] M. Koenig et al., Science **318**, 766 (2007).

[21] D. Hsieh et al., Science **323**, 919 (2009).

[22] D. Hsieh et al., Phys. Rev. Lett. **103**, 146401 (2009).

[23] M. A. Brand et al., Phys. Rev. Lett. **89**, 236601 (2002).

[24] C. Weber et al., Nature **437**, 1330 (2005).

[25] J. D. Koralek et al., Nature **458**, 610 (2009).

[26] M. I. D'Yakonov and V. I. Perel', Soviet Journal of Experimental and Theoretical Physics Letters **13**, 467 (1971).

[27] M. I. D'Yakonov and V. I. Perel', Soviet Journal of Experimental and Theoretical Physics **33**, 1053 (1971).

[28] M. I. D'Yakonov and V. I. Perel', Soviet physics: Semiconductors **20**, 110 (1986).

[29] F. Meier and B. P. Zakharchenya, *Optical orientation (Modern Problems in Condensed Matter Sciences)*, North-Holland, 1984.

[30] A. A. Burkov, A. S. Núñez, and A. H. MacDonald, Phys. Rev. B **70**, 155308 (2004).

[31] E. G. Mishchenko, A. V. Shytov, and B. I. Halperin, Phys. Rev. Lett. **93**, 226602 (2004).

[32] A. Punnoose and A. M. Finkel'stein, Phys. Rev. Lett. **96**, 057202 (2006).

[33] T. D. Stanescu and V. Galitski, Phys. Rev. B **75**, 125307 (2007).

[34] J. H. Jiang and M. W. Wu, Phys. Rev. B **79**, 125206 (2009).

[35] L. Yang, J. Orenstein, and D.-H. Lee, Phys. Rev. B **82**, 155324 (2010).

[36] W. J. H. Leyland et al., Phys. Rev. B **76**, 195305 (2007).

[37] C. P. Weber et al., Phys. Rev. Lett. **98**, 076604 (2007).

[38] E. Akkermans and G. Montambaux, *Mesoscopic Physics of Electrons and Photons*, Cambridge University Press, 2007.

[39] A. G. Mal'shukov, K. A. Chao, and M. Willander, Phys. Rev. Lett. **76**, 3794 (1996).

[40] I. S. Lyubinskiy and V. Y. Kachorovskii, Phys. Rev. B **70**, 205335 (2004).

[41] E. I. Rashba, Sov. Phys. Solid State **2**, 1109 (1960).

[42] Y. A. Bychkov and E. I. Rashba, Journal of Physics C: Solid State Physics **17**, 6039 (1984).

[43] G. Dresselhaus, Phys. Rev. **100**, 580 (1955).

[44] B. A. Bernevig and J. Hu, Phys. Rev. B **78**, 245123 (2008).

[45] M. Glazov and E. Ivchenko, JETP Letters **75**, 403 (2002), 10.1134/1.1490009.

[46] I. D'Amico and G. Vignale, Phys. Rev. B **68**, 045307 (2003).

[47] B. A. Bernevig, J. Orenstein, and S.-C. Zhang, Phys. Rev. Lett. **97**, 236601 (2006).

[48] L. Zheng and S. Das Sarma, Phys. Rev. B **53**, 9964 (1996).

[49] I. D'Amico and G. Vignale, Phys. Rev. B **62**, 4853 (2000).

[50] J. Rammer and H. Smith, Rev. Mod. Phys. **58**, 323 (1986).

[51] X. Liu, X.-J. Liu, and J. Sinova, Phys. Rev. B **84**, 035318 (2011).

[52] J. Rammer, *Quantum Field Theory of Non-equilibrium States*, Cambridge University Press, 2007.

[53] M. Schütt, P. M. Ostrovsky, I. V. Gornyi, and A. D. Mirlin, Phys. Rev. B **83**, 155441 (2011).

[54] R. Winkler, *Spin-orbit Coupling Effects in Two-Dimensional Electron and Hole Systems*, Springer, 2003.

[55] R. J. Elliott, Phys. Rev. **96**, 266 (1954).

[56] Y. Yafet, *Solid State Physics*, volume 14, Academic, New York, 1963.

[57] Nozières, P. and Lewiner, C., J. Phys. France **34**, 901 (1973).

[58] I. Zutic, J. Fabian, and S. Das Sarma, Rev. Mod. Phys. **76**, 323 (2004).

[59] P. Boguslawski, Solid State Communications **33**, 389 (1980).

[60] P. I. Tamborenea, M. A. Kuroda, and F. L. Bottesi, Phys. Rev. B **68**, 245205 (2003).

APPENDIX A

SPIN DYNAMIC THEORY FROM LINEAR RESPONSE THEORY

A.1 Spin dynamic matrix for the uniform spin polarization

In this section, we derive the spin evolution mode of the uniform spin polarization. According to Eq. (3.5) the strength of SOI is angle dependent and can be written as

$$\mathrm{h}_{so} = \sqrt{\alpha^2+\beta_1^2}k_f \times$$
$$\sqrt{1+(2(\tfrac{\beta_3}{\lambda'})^2 - \tfrac{2\beta_3}{\lambda'}\sin(\psi+\pi/4))(1+\cos 4\theta) + (\cos 2\psi - \tfrac{4\beta_3}{\lambda'}\cos(\psi+\pi/4))\cos 2\theta}$$

where $\cos\psi = \lambda_1/\sqrt{\lambda_1^2+\lambda_2^2}$.

First we consider the case for $\beta_3 = 0$. The Hamiltonian is written as

$$\begin{aligned} H &= \frac{k^2}{2m} + (\alpha+\beta)k_x\sigma_y - (\alpha-\beta)k_y\sigma_x, \\ &= \frac{k^2}{2m} + \lambda_1 k_x\sigma_y + \lambda_2 k_y\sigma_x, \end{aligned} \tag{A.1}$$

where k_x is along the [110] direction, $\lambda_1 = \alpha+\beta$ and $\lambda_2 = -(\alpha-\beta)$. The Green's function for this Hamiltonian takes the form

$$\begin{aligned} G^{R(A)} &= \frac{E - \frac{k^2}{2m} \pm \frac{i}{2\tau} + (\alpha+\beta)k_x\sigma_y - (\alpha-\beta)k_y\sigma_x}{(E-\frac{k^2}{2m}\pm\frac{i}{2\tau})^2 - (\alpha^2+\beta^2)k^2(1+\frac{2\alpha\beta}{\alpha^2+\beta^2}\cos 2\theta)} \\ &= \frac{E - \frac{k^2}{2m} \pm \frac{i}{2\tau} + \lambda_1 k_x\sigma_y + \lambda_2 k_y\sigma_x}{(E-\frac{k^2}{2m}\pm\frac{i}{2\tau})^2 - \frac{(\lambda_1^2+\lambda_2^2)}{2}k^2(1+\gamma\cos 2\theta)}, \end{aligned} \tag{A.2}$$

where τ is the momentum scattering time, $\gamma = \frac{2\alpha\beta}{\alpha^2+\beta^2} = \frac{\lambda_1^2-\lambda_2^2}{\lambda_1^2+\lambda_2^2}$. It is more convenient to write down the element of the 2×2 Green's function Eq. (A.2) as

$$\begin{aligned}
G_{11} &= G_{22} = \frac{1}{2(E - \frac{k^2}{2m} - \lambda k\sqrt{1+\gamma\cos 2\theta} \pm \frac{i}{\tau})} \\
&\quad + \frac{1}{2(E - \frac{k^2}{2m} + \lambda k\sqrt{1+\gamma\cos 2\theta} \pm \frac{i}{\tau})}, \\
G_{12} &= \frac{1}{2}\left(\frac{1}{E - \frac{k^2}{2m} - \lambda k\sqrt{1+\gamma\cos 2\theta} \pm \frac{i}{\tau}} - \frac{1}{E - \frac{k^2}{2m} + \lambda k\sqrt{1+\gamma\cos 2\theta} \pm \frac{i}{\tau}}\right) \times \\
&\quad \frac{\sqrt{2}(-i\cos\psi\cos\theta + \sin\psi\sin\theta)}{\sqrt{1+\gamma\cos 2\theta}} \\
G_{21} &= \frac{1}{2}\left(\frac{1}{E - \frac{k^2}{2m} - \lambda k\sqrt{1+\gamma\cos 2\theta} \pm \frac{i}{\tau}} - \frac{1}{E - \frac{k^2}{2m} + \lambda k\sqrt{1+\gamma\cos 2\theta} \pm \frac{i}{\tau}}\right) \times \\
&\quad \frac{\sqrt{2}(i\cos\psi\cos\theta + \sin\psi\sin\theta)}{\sqrt{1+\gamma\cos 2\theta}}
\end{aligned} \tag{A.3}$$

where $\lambda = \sqrt{(\lambda_1^2+\lambda_2^2)/2} = \sqrt{\alpha^2+\beta^2}$, $\cos\psi = \lambda_1/\sqrt{\lambda_1^2+\lambda_2^2}$ and $\gamma = \cos 2\psi$.

According to Eq. (2.8), the diagonal element of the spin polarization along z direction has the form

$$\begin{aligned}
I^{zz} &= I_{11,11} - I_{11,22} - I_{22,11} + I_{22,22} \\
&= \frac{1}{2m\tau}\int \frac{d^2k}{(2\pi)^2}(G_{11}^A G_{11}^R - G_{21}^A G_{12}^R - G_{12}^A G_{21}^R + G_{22}^A G_{22}^R).
\end{aligned} \tag{A.4}$$

The first term and the fourth term in Eq. (A.4) are equal to each other and have the form

$$\frac{1}{2m\tau}\int \frac{d^2k}{(2\pi)^2} G_{11}^A G_{11}^R = \frac{1}{2m}\int \frac{d^2k}{(2\pi)^2}\frac{1}{4}\left(\frac{1}{E - \epsilon_+(k) - \frac{i}{2\tau}} + \frac{1}{E - \epsilon_-(k) - \frac{i}{2\tau}}\right) \times$$

$$
\begin{aligned}
& (\frac{1}{E+\Omega-\epsilon_-(k)+\frac{i}{2\tau}}+\frac{1}{E+\Omega-\epsilon_-(k)+\frac{i}{2\tau}}) \\
= & \frac{1}{16m\pi}\int_0^{2\pi}\frac{d\theta}{v_f}(\frac{k^+}{1-i\Omega\tau}+\frac{k^-}{1-i\Omega\tau+2i\lambda k\sqrt{1+\gamma\cos 2\theta}} \\
& +\frac{k^+}{1-i\Omega\tau-2i\lambda k\sqrt{1+\gamma\cos 2\theta}}+\frac{k^-}{1-i\Omega\tau}), \\
\simeq & \frac{1}{16\pi}\int_0^{2\pi}d\theta(\frac{1}{1-i\Omega\tau}+\frac{1}{1-i\Omega\tau+2i\lambda k\sqrt{1+\gamma\cos 2\theta}} \\
& +\frac{1}{1-i\Omega\tau-2i\lambda k\sqrt{1+\gamma\cos 2\theta}}+\frac{1}{1-i\Omega\tau}),
\end{aligned}
\tag{A.5}
$$

where $v_f=\frac{\partial E_f}{\partial k}$. In the polar coordinate, $\int d^2k=\int d(k^2/2)d\theta$. As we assume that $\lambda k_f \ll E_f$, $d(k^2/2)\simeq mdE$ where m is the effective mass.

The other two terms are also equal to each other and can be written as

$$
\begin{aligned}
\frac{1}{2m\tau}\int\frac{d^2k}{(2\pi)^2}G_{21}^AG_{12}^R = & \int\frac{d^2k}{(2\pi)^2}\frac{1}{4}(\frac{1}{E-\epsilon_+(k)-\frac{i}{2\tau_e}}-\frac{1}{E-\epsilon_-(k)-\frac{i}{2\tau_e}})\times \\
& (\frac{1}{E+\Omega-\epsilon_+(k)+\frac{i}{2\tau_e}}-\frac{1}{E+\Omega-\epsilon_-(k)+\frac{i}{2\tau_e}}) \\
= & \frac{1}{16m\pi}\int_0^{2\pi}\frac{d\theta}{v_f}(\frac{k^+}{1-i\Omega\tau}-\frac{k^-}{1-i\Omega\tau+2i\lambda k\sqrt{1+\gamma\cos 2\theta}} \\
& -\frac{k^+}{1-i\Omega\tau-2i\lambda k\sqrt{1+\gamma\cos 2\theta}}+\frac{k^-}{1-i\Omega\tau}) \\
\simeq & \frac{1}{16\pi}\int_0^{2\pi}d\theta(\frac{1}{1-i\Omega\tau}-\frac{1}{1-i\Omega\tau+2i\lambda k\sqrt{1+\gamma\cos 2\theta}} \\
& -\frac{1}{1-i\Omega\tau-2i\lambda k\sqrt{1+\gamma\cos 2\theta}}+\frac{1}{1-i\Omega\tau},
\end{aligned}
\tag{A.6}
$$

Substituting Eqs. (A.5 ,A.6) to Eq. (A.4), we have

$$
\begin{aligned}
I^{zz} &= \frac{1}{4\pi}\int_0^{2\pi} d\theta\left(\frac{1}{1-i\Omega\tau+2i\lambda k\sqrt{1+\gamma\cos 2\theta}}+\frac{1}{1-i\Omega\tau-2i\lambda k\sqrt{1+\gamma\cos 2\theta}}\right)\\
&= \frac{1}{2\pi}\int_0^{2\pi} d\theta\frac{1-i\Omega\tau}{(1-i\Omega\tau)^2+(\Omega_{so}\tau)^2(1+\gamma\cos 2\theta)}\\
&= \frac{1-i\Omega\tau}{2\pi((1-i\Omega\tau)^2+(\Omega_{so}\tau)^2)}\int_0^{\pi} dx\frac{2}{(1+a\cos(x))},
\end{aligned}
\tag{A.7}
$$

where $x=2\theta$ and $a=\gamma(\Omega_{so}\tau)^2/((1-i\Omega\tau)^2+(\Omega_{so}\tau)^2)$. The indefinite integral $\int dx\frac{1}{1+a\cos(x)}=\frac{2arc\tanh\left[\frac{(-1+a)\tan\left[\frac{x}{2}\right]}{\sqrt{-1+a^2}}\right]}{\sqrt{-1+a^2}}$. Therefore we have

$$
\begin{aligned}
I^{zz} &= \frac{1-i\Omega\tau}{2\pi((1-i\Omega\tau)^2+(\Omega_{so}\tau)^2)}\int_0^{\pi} dx\frac{2}{(1+a\cos(x))}\\
&= \frac{1-i\Omega\tau}{2\pi((1-i\Omega\tau)^2+(\Omega_{so}\tau)^2)}\\
&\quad\times 2\left(\frac{2arc\tanh\left[\frac{(-1+a)\tan\left[\frac{\pi}{2}\right]}{\sqrt{-1+a^2}}\right]}{\sqrt{-1+a^2}}-\frac{2arc\tanh\left[\frac{(-1+a)\tan\left[\frac{0}{2}\right]}{\sqrt{-1+a^2}}\right]}{\sqrt{-1+a^2}}\right)\\
&= \frac{1-i\Omega\tau}{2\pi((1-i\Omega\tau)^2+(\Omega_{so}\tau)^2)}\times\frac{2\pi i}{\sqrt{-1+a^2}}\\
&= \frac{1-i\Omega\tau}{\sqrt{((1-i\Omega\tau)^2+(\Omega_{so}\tau)^2)^2-\gamma^2(\Omega_{so}\tau)^4}}.
\end{aligned}
\tag{A.8}
$$

When Rashba SOI is zero, the strength of SOIs takes the form

$$
h_{so}=\beta_1 k_f\sqrt{1+(2\frac{\beta_3^2}{\beta_1^2}-2\frac{\beta_3}{\beta_1})(1+\cos 4\theta)}.
\tag{A.9}
$$

To obtain the spin diffusive matrix element I^{zz}, it is easy to prove that we only need to replace the term $\lambda k\sqrt{1+\gamma\cos 2\theta}$ in Eq. (A.8) with h_{so} in Eq. (A.9). Therefore, we have

$$\begin{aligned} I^{zz} &= \frac{1}{4\pi}\int(\frac{2(1-i\Omega\tau)}{(1-i\Omega\tau)^2+(2h_{so}\tau)^2})d\theta \\ &= \frac{1-i\Omega\tau}{\sqrt{(1-i\Omega\tau)^2+\Omega_{so}^2\tau^2}\sqrt{(1-i\Omega\tau)^2+\Omega_{so}^2\tau^2(1+2(\frac{\beta_3}{\beta_1})^2-2\frac{\beta_3}{\beta_1})}}. \end{aligned} \quad \text{(A.10)}$$

APPENDIX B

SPIN DYNAMIC THEORY FROM KELDYSH FORMALISM

B.1 Elliott-Yafet mechanism

In this appendix, we will discuss the spin relaxation due to the Elliott-Yafet (55; 56) mechanism in the III-V semiconductor quantum well. There are two processes involved: the Elliott process and (55) and the Yafet process. (56). In the Yafet process, the spin flip is due to the intrinsic spin-orbit coupling of the scattering potential which has the well know form

$$H_{so}^{intri} = -\frac{\hbar^2}{4m_0^2c^2}\boldsymbol{\sigma}\cdot(\boldsymbol{k}\times\boldsymbol{\nabla}V), \tag{B.1}$$

where m_0 is the electron mass in the free space and V is the scattering potential which can be impurity, e-ph and e-e scattering. Here to estimate the strength of the Yafet process, we assume $V(\boldsymbol{r})$ is a spherical potential which is independent on the direction. In this case, the SOC Hamiltonian is Eq. B.1 is simplified to be

$$\begin{aligned} H_{so}^{intri} &= \frac{\hbar^2}{4m_0^2c^2}\boldsymbol{\sigma}(\boldsymbol{k}\times\boldsymbol{e_r}\partial_r V(r) \\ &= -\frac{\hbar^2}{4m_0^2c^2}\frac{\partial_r V(r)}{r}(\boldsymbol{r}\times\boldsymbol{k})\cdot\boldsymbol{\sigma} = -\frac{\hbar^2}{4m_0^2c^2}\frac{\partial_r V(r)}{r}(\boldsymbol{L}\cdot\boldsymbol{\sigma}) \\ &= -\frac{\hbar^2}{4m_0^2c^2}\frac{\partial_r V(r)}{r}\frac{j(j+1)-l(l+1)-s(s+1)}{2}, \end{aligned} \tag{B.2}$$

where $\boldsymbol{L}$ is the orbital angular momentum, $j(l,s)$ is the quantum number of the total angular momentum (orbital angular momentum, spin). In the Γ_7^- of the III-V semiconductors, $j = 3/2$, $l = 1$ and $s = 1/2$. Therefore the expectation value of H_{so}^{intri} in Γ_7^- can be written as

$$\begin{aligned} \overline{H}_{so}^{\Gamma_8^v} &= \langle j = \frac{3}{2}, l = 1 | H_{so} | j = \frac{3}{2}, l = 1 \rangle = -\frac{\hbar^2}{4m_0^2c^2} \langle \frac{\partial_r V(r)}{r} \rangle \frac{1}{2} \\ &= \frac{\hbar^2}{4m_0^2c^2} \langle \frac{V(r)}{r^2} \rangle \frac{1}{2} \approx \frac{\hbar^2}{4m_0^2c^2(a_0/2)^2} \frac{\overline{V}}{2}, \end{aligned} \tag{B.3}$$

where a_0 is the lattice constant. Here we assume that $\langle 1/r^2 \rangle = 4/a_0^2$. Similar, in the Γ_7^v band, $\overline{H}_{so}^{\Gamma_7^v} = -\frac{\hbar^2}{m_0^2c^2a_0^2}\overline{V}$ and in the Γ_6^c, $\overline{H}_{so}^{\Gamma_6^c} = 0$.

In the Elliott process, the spin flip is due to the spin-orbit interaction (SOI) on the Bloch state, say the eigenstate of the electron in the conduction band is not the spin eigenstate. However the momentum scattering potential is $\overline{V}$ which is spin independent. From this viewpoint, the Elliott process has the same origination with the Rashba SOI in the III-V semiconductor quantum well. The difference lies the fact that in the Rashba SOI, the electric field along z direction break the inversion symmetry and the first non-zero term of Rashb SOI is linear dependent on the wave vector $\boldsymbol{k}$ of the conduction electrons which make the spin up and spin down states with the same momentum k are note degenerate any more. In the Elliott processes, the scattering potential does not break the inversion symmetry, its nonzer terms is

proportional to k^2 and spin up and spin down electrons with the same momentum is still degenerate.

After talk about the origination of both Elliott and Yafet mechanism, based on the 8×8 Kane model, the effective Hamiltonian of the electrons in the conduction band of III-V semiconductors such as GaAs has the form

$$\begin{aligned} \hat{H}_c &= \frac{P^2}{3}\left[\frac{2}{E_0} + \frac{1}{E_0+\Delta_0}\right]k^2 - \frac{P^2}{3}\left[\frac{1}{E_0^2} - \frac{1}{(E_0+\Delta_0)^2}\right]\boldsymbol{\sigma}\cdot\boldsymbol{\nabla}V\times\mathbf{k} \\ &+ \frac{P^2}{3}\left[\frac{1}{E_0^2} + \frac{1}{(E_0+\Delta_0)^2}\right]\frac{\hbar^2}{2m_0^2c^2a_0^2}\boldsymbol{\sigma}\cdot\boldsymbol{\nabla}V\times\mathbf{k}, \end{aligned} \tag{B.4}$$

where V is the spin independent scattering potential, $P = \frac{i\hbar^2}{m_0} < S|\nabla|R >$, $|S\rangle$ is the s-wave like local orbital state, $R = X, Y, Z$ are the p-wave like local orbital states, E_0 is the energy gap between Γ_6^- and Γ_8^+ bands and Δ_0 is the energy gap between Γ_8^+ and Γ_7^+ bands (54). The second term in Eq. B.4 is corresponding to the Elliott spin relaxation mechanism and vanish when the SOC gap $\Delta_0 = 0$. The third term in Eq. B.4 is corresponding to the Yafet spin relaxation mechanism which will not vanish when the SOC gap $\Delta_0 = 0$. These are consistent to the characters of Elliott and Yafet mechanisms. For Elliott spin relaxation mechanism, the scattering potential is spin independent, therefore only the SOC gap Δ_0 can provide the necessary SOI to relax spin. In Yafet mechanism, the scattering potential itself contains SOC whic can make spin relax. Therefore the SOC gap Δ_0 is not necessary in this case.

Now, let us compare the strength of the Elliott and Yafet mechanism in the GaAs 2DQW, where $P = 10.493\text{eV}\text{Å}$, the band gaps $E_0 = 1.519$ eV $\Delta_0 = 0.341$ eV (54). Therefore, in the III-V semiconductors, the ration between the Elliot and Yafet mechanism is at the order of

$$\frac{\left[\frac{1}{E_0^2} - \frac{1}{(E_0+\Delta_0)^2}\right]}{\left[\frac{1}{E_0^2} + \frac{1}{(E_0+\Delta_0)^2}\right]\left[\frac{\hbar^2}{2m_0^2c^2a_0^2}\right]} = 4.84 \times 10^5, \tag{B.5}$$

which indicates that the Elliot spin relaxation is much larger than the Yafet spin relaxation. Therefore, in the following derivation , we only focus on the Elliot mechanism. The first term in the Eq. B.4 is the normal kinetic energy and the second term is the SOC terms In 2D quantum well, by applying an electric potential along z direction $V_z = -eEz$, the inversion symmetry is broken and $< \boldsymbol{\nabla} V_z >$ is nonzero which gives the Rashba SOC. However, in the Elliott process, the potential V is from the impurity scattering, electron-phonon (55) and electron-electron interaction (60), the average, $\langle \boldsymbol{\nabla} V \rangle$, is zero. Therefore the first nonzero term of Elliott process is proportional to $(\langle \boldsymbol{\nabla} V \rangle)^2$. The spin-orbit coupling potential can be written in the momentum space as (38)

$$\begin{aligned}
\hat{V}_{so}(k,k') &= i\gamma V(\boldsymbol{k} \times \boldsymbol{k'}) \cdot \boldsymbol{\sigma} \\
&= i\gamma V \left\{(k_x k'_y - k_y k'_x)\sigma_z + (k_y k'_z - k_z k'_y)\sigma_x + (k_z k'_x - k_x k'_z)\sigma_y\right\} \\
&= i(V^z\sigma_z + V^x\sigma_x + V^y\sigma_y),
\end{aligned} \tag{B.6}$$

where k' and k are the momentums of the electrons before and after scattering respectively, $\gamma = \frac{P^2}{3}(\frac{1}{E_0^2} - \frac{1}{(E_0+\Delta_0)^2})$ and V is the momentum scattering potential.

Before we calculate the Elliott mechanism, let us connect the quantum kinetic equation to the continuous equation by integrating the momentum $\boldsymbol{k}$. To simplify our argument, we consider the case where the SOC due to the inversion asymmetry is zero. Eq. 3.8 after the integral has the form

$$\begin{aligned} & \partial_T \hat{\rho}(E, \boldsymbol{R}, T) + \boldsymbol{\nabla} \cdot \hat{\boldsymbol{J}}(E, \boldsymbol{R}, T) \\ = & \int \frac{d^2k}{(2\pi)^2} \left[(\Sigma^R G^K + \Sigma^K G^A) - (G^R \Sigma^K + G^K \Sigma^A) \right]. \end{aligned} \tag{B.7}$$

Eq. B.7 is the continuous equation in the spin-$\frac{1}{2}$ basis. Multiply $\mathrm{Tr}\sigma_\mathrm{m}/2$ on both sides of Eq. B.7 we have the traditional continuous equation

$$\partial_T \rho_m + \boldsymbol{\nabla} \cdot \boldsymbol{J}_m = \int \frac{d^2k}{(2\pi)^2} \mathrm{Tr} \frac{\sigma_\mathrm{m}}{2} \left[(\Sigma^\mathrm{R} \mathrm{G}^\mathrm{K} + \Sigma^\mathrm{K} \mathrm{G}^\mathrm{A}) - (\mathrm{G}^\mathrm{R} \Sigma^\mathrm{K} + \mathrm{G}^\mathrm{K} \Sigma^\mathrm{A}) \right], \tag{B.8}$$

where $m = 0, x, y, z$ are corresponding to charge, spin-x, spin-y and spin-z respectively. If the charge or spin is conserved, the scattering term on the right hand side of Eq. B.8 is zero. Now let us substitute the SOC potential to the scattering term. There are four terms in the collision integral and we first focus on the two terms containing the retarded Green's function or self energy which has the form

$$\int \frac{d^2k}{(2\pi)^2} \mathrm{Tr} \frac{1}{2} \left\{ \sigma_\mathrm{m} (\hat{\Sigma}^\mathrm{R} \hat{\mathrm{G}}^\mathrm{K} - \hat{\mathrm{G}}^\mathrm{R} \hat{\Sigma}^\mathrm{K}) \right\}$$

$$
\begin{aligned}
&= \mathrm{Tr}\left\{\int \frac{\mathrm{d}^2\mathrm{k}'}{(2\pi)^2}\frac{\sigma_\mathrm{m}}{2}\left[\hat{\mathrm{V}}_{\mathrm{kk}'}\mathrm{G}^\mathrm{R}(\mathrm{k}')\hat{\mathrm{V}}_{\mathrm{k}'\mathrm{k}}\mathrm{G}^\mathrm{K}(\mathrm{k}) - \mathrm{G}^\mathrm{R}(\mathrm{k})\hat{\mathrm{V}}_{\mathrm{kk}'}\mathrm{G}^\mathrm{K}(\mathrm{k}')\hat{\mathrm{V}}_{\mathrm{k}'\mathrm{k}}\right]\right\} \\
&= \mathrm{Tr}\left\{\int \frac{\mathrm{d}^2\mathrm{k}}{(2\pi)^2}\frac{\mathrm{d}^2\mathrm{k}'}{(2\pi)^2}(\frac{\sigma_\mathrm{m}}{2}\hat{\mathrm{V}}_{\mathrm{kk}'} - \hat{\mathrm{V}}_{\mathrm{kk}'}\frac{\sigma_\mathrm{m}}{2})\mathrm{G}^\mathrm{R}(\mathrm{k}')(\hat{\mathrm{V}}_{\mathrm{k}'\mathrm{k}})\mathrm{G}^\mathrm{K}(\mathrm{k})\right\} \\
&+ \mathrm{Tr}\left\{\int \frac{\mathrm{d}^2\mathrm{k}}{(2\pi)^2}\frac{\mathrm{d}^2\mathrm{k}'}{(2\pi)^2}\frac{\sigma_\mathrm{m}}{2}(\mathrm{G}^\mathrm{R}(\mathrm{k}')\hat{\mathrm{V}}_{\mathrm{k}'\mathrm{k}}\hat{\mathrm{G}}^\mathrm{K}(\mathrm{k})\hat{\mathrm{V}}_{\mathrm{kk}'} - \mathrm{G}^\mathrm{R}(\mathrm{k})\hat{\mathrm{V}}_{\mathrm{kk}'}\hat{\mathrm{G}}^\mathrm{K}(\mathrm{k}')\hat{\mathrm{V}}_{\mathrm{k}'\mathrm{k}})\right\} \qquad \text{(B.9)}
\end{aligned}
$$

The last term on the right hand side of Eq. B.9 is zero because the symmetric places of k and k' in this term. The first term on the right hand side of Eq. B.9 can be written further as

$$
\begin{aligned}
&\mathrm{Tr}\left\{\int \frac{\mathrm{d}^2\mathrm{k}'}{(2\pi)^2}(\frac{\sigma_\mathrm{m}}{2}\hat{\mathrm{V}}_{\mathrm{kk}'} - \hat{\mathrm{V}}_{\mathrm{kk}'}\frac{\sigma_\mathrm{m}}{2})\mathrm{G}^\mathrm{R}(\mathrm{k}')(\hat{\mathrm{V}}_{\mathrm{k}'\mathrm{k}})\mathrm{G}^\mathrm{K}(\mathrm{k})\right\} \\
&= \mathrm{Tr}\left\{\int \frac{\mathrm{d}^2\mathrm{k}'}{(2\pi)^2}[\frac{\sigma_\mathrm{m}}{2}, \mathrm{V}^\mathrm{j}\sigma^\mathrm{j}]\mathrm{G}^\mathrm{R}(\mathrm{k}')(\hat{\mathrm{V}}_{\mathrm{k}'\mathrm{k}})\mathrm{G}^\mathrm{K}(\mathrm{k})\right\} \\
&= \mathrm{Tr}\left\{\int \frac{\mathrm{d}^2\mathrm{k}'}{(2\pi)^2}2\mathrm{i}\epsilon_{\mathrm{mjk}}\mathrm{V}^\mathrm{j}_{\mathrm{kk}'}\frac{\sigma_\mathrm{k}}{2}\mathrm{G}^\mathrm{R}(\mathrm{k}')(\hat{\mathrm{V}}_{\mathrm{k}'\mathrm{k}})\mathrm{G}^\mathrm{K}(\mathrm{k})\right\} \\
&= \mathrm{Tr}\left\{\int \frac{\mathrm{d}^2\mathrm{k}'}{(2\pi)^2}(-4)\epsilon_{\mathrm{mjk}}\epsilon_{\mathrm{kjm}}\mathrm{V}^\mathrm{j}_{\mathrm{kk}'}\mathrm{V}^\mathrm{j}_{\mathrm{k}'\mathrm{k}}\frac{\sigma_\mathrm{m}}{2}\mathrm{G}^\mathrm{R}(\mathrm{k}')\mathrm{G}^\mathrm{K}(\mathrm{k})\right\} \\
&= \mathrm{Tr}\left\{\int \frac{\mathrm{d}^2\mathrm{k}'}{(2\pi)^2}4(\sum_{\mathrm{j}\neq\mathrm{m}}\mathrm{V}^\mathrm{j}_{\mathrm{kk}'}\mathrm{V}^\mathrm{j}_{\mathrm{k}'\mathrm{k}})\frac{\sigma_\mathrm{m}}{2}\mathrm{G}^\mathrm{R}(\mathrm{k}')\mathrm{G}^\mathrm{K}(\mathrm{k})\right\}, \qquad \text{(B.10)}
\end{aligned}
$$

For the charge dynamics, we need take $m = 0$. Because σ_0 commutes with any scattering potential operator, the Eq. B.10 is always zero which indicates that the charge is always conserved. For the spin dynamics, $m = x, y, z$. Generally speaking, $\sigma_{x(y,z)}$ do not commutes with a spin dependent scattering potential and the Eq. B.10

is nonzero which indicates that the spin will decay. It is noted that in the 2DEG, k_z is quantized. Therefore, taking $m = x, y, z$ we have

$$\begin{aligned}
&\mathrm{Tr}\left\{\int \frac{\mathrm{d}^2\mathrm{k}'}{(2\pi)^2} 4(\sum_{\mathrm{j}\neq\mathrm{x}} \mathrm{V}^{\mathrm{j}}_{\mathrm{kk}'}\mathrm{V}^{\mathrm{j}}_{\mathrm{k}'\mathrm{k}})\frac{\sigma_{\mathrm{x}}}{2}\mathrm{G}^{\mathrm{R}}(\mathrm{k}')\mathrm{G}^{\mathrm{K}}(\mathrm{k})\right\} \\
= \; & -i\frac{\gamma^2 k_F^4}{\tau_p}(1+\frac{2k_z^2}{k_F^2})G_x^K = -iA(1+\frac{2\langle k_z^2\rangle}{k_F^2})\left(\frac{\Delta_0}{E_0+\Delta_0}\right)^2\left(\frac{\epsilon_k}{E_0}\right)^2\frac{G_x^K}{2\tau_p}, \\
&\mathrm{Tr}\left\{\int \frac{\mathrm{d}^2\mathrm{k}'}{(2\pi)^2} 4(\sum_{\mathrm{j}\neq\mathrm{y}} \mathrm{V}^{\mathrm{j}}_{\mathrm{kk}'}\mathrm{V}^{\mathrm{j}}_{\mathrm{k}'\mathrm{k}})\frac{\sigma_{\mathrm{y}}}{2}\mathrm{G}^{\mathrm{R}}(\mathrm{k}')\mathrm{G}^{\mathrm{K}}(\mathrm{k})\right\} \\
= \; & -i\frac{\gamma^2 k_F^4}{\tau_p}(1+\frac{2k_z^2}{k_F^2})G_y^K = -iA(1+\frac{2\langle k_z^2\rangle}{k_F^2})\left(\frac{\Delta_0}{E_0+\Delta_0}\right)^2\left(\frac{\epsilon_k}{E_0}\right)^2\frac{G_x^K}{2\tau_p}, \\
&\mathrm{Tr}\left\{\int \frac{\mathrm{d}^2\mathrm{k}'}{(2\pi)^2} 4(\sum_{\mathrm{j}\neq\mathrm{z}} \mathrm{V}^{\mathrm{j}}_{\mathrm{kk}'}\mathrm{V}^{\mathrm{j}}_{\mathrm{k}'\mathrm{k}})\frac{\sigma_{\mathrm{z}}}{2}\mathrm{G}^{\mathrm{R}}(\mathrm{k}')\mathrm{G}^{\mathrm{K}}(\mathrm{k})\right\} \\
= \; & -i\frac{\gamma^2 k_F^4}{\tau_p}\frac{4k_z^2}{k_F^2}G_z^K = -iA\frac{4k_z^2}{k_F^2}\left(\frac{\Delta_0}{E_0+\Delta_0}\right)^2\left(\frac{\epsilon_k}{E_0}\right)^2\frac{G_z^K}{2\tau_p},
\end{aligned} \tag{B.11}$$

where $k_z = \pi/d$ and d is the width of the quantum well and A is the order of 1. The other two terms, containing the advance Green's function in Eq. B.8, gives the same result to the Eq. B.11 It is noted that the average, $\langle k_z^2\rangle$, is nonzero which is also the reason why there is the linear Dresselhaus term in the III-V semiconductor quantum well. Therefore, although average $\langle k_z\rangle$ is zero, the components of Elliott mechanism which are proportional to the $\langle k_z^2\rangle$ are still finite. As a result, the Elliott spin relaxation rates have the form

$$\begin{aligned}
\frac{1}{\tau_{EY,x}} = \frac{1}{\tau_{EY,y}} &= A(1+\frac{2\langle k_z^2\rangle}{k_F^2})\left(\frac{\Delta_0}{E_0+\Delta_0}\right)^2\left(\frac{\epsilon_k}{E_0}\right)^2\frac{1}{\tau_p} = \frac{\kappa_1}{\tau_p}, \\
\frac{1}{\tau_{EY,z}} &= A\frac{4\langle k_z^2\rangle}{k_F^2}\left(\frac{\Delta_0}{E_0+\Delta_0}\right)^2\left(\frac{\epsilon_k}{E_0}\right)^2\frac{1}{\tau_p} = \frac{\kappa_1^{\perp}}{\tau_p},
\end{aligned} \tag{B.12}$$

The same result can be obtained from the traditional definition of the spin decay rate due to the admixture of the Pauli spin up and spin down in the eigenstates of the conduction electron. From the 8×8 Kane mode we can obtain these eigenstates as

$$\begin{aligned}
\Psi_{ck,\uparrow} &= |S,\uparrow\rangle + \frac{-1}{\sqrt{2}}\frac{P}{E_0}k_+|\frac{3}{2},\frac{3}{2}\rangle + \sqrt{\frac{2}{3}}\frac{P}{E_0}k_z|\frac{3}{2},\frac{1}{2}\rangle + \frac{1}{\sqrt{6}}\frac{P}{E_0}k_-|\frac{3}{2},-\frac{1}{2}\rangle \\
&\quad + \frac{-1}{\sqrt{3}}\frac{P}{E_0+\Delta_0}k_z|\frac{1}{2},\frac{1}{2}\rangle + \frac{-1}{\sqrt{3}}\frac{P}{E_0+\Delta_0}k_-|\frac{1}{2},-\frac{1}{2}\rangle, \\
\Psi_{ck,\downarrow} &= |S,\downarrow\rangle + \frac{-1}{\sqrt{6}}\frac{P}{E_0}k_+|\frac{3}{2},\frac{1}{2}\rangle + \sqrt{\frac{2}{3}}\frac{P}{E_0}k_z|\frac{3}{2},-\frac{1}{2}\rangle + \frac{1}{\sqrt{2}}\frac{P}{E_0}k_-|\frac{3}{2}, \\
&\quad -\frac{3}{2}\rangle + \frac{-1}{\sqrt{3}}\frac{P}{E_0+\Delta_0}k_+|\frac{1}{2},\frac{1}{2}\rangle + \frac{1}{\sqrt{3}}\frac{P}{E_0+\Delta_0}k_z|\frac{1}{2},-\frac{1}{2}\rangle.
\end{aligned} \tag{B.13}$$

The transition amplitude between these two states with different wave vector k are proportional to

$$\begin{aligned}
\langle\Psi_{ck',\downarrow}|V(\boldsymbol{r})|\Psi_{ck,\uparrow}\rangle &= V_0\left(-\frac{1}{3}\frac{P^2}{E_0^2}(k_zk'_- - k_-k'_z) + \frac{1}{3}\frac{P^2}{(E_0+\Delta_0)^2}(k_zk'_- - k_-k'_z)\right) \\
&= V_0\left(-\frac{1}{3}(k_zk'_- - k_-k'_z)(\frac{P^2}{E_0^2} - \frac{P^2}{(E_0+\Delta_0)^2})\right) \\
&= -V_0\gamma(k_zk'_- - k_-k'_z).
\end{aligned} \tag{B.14}$$

Therefore the spin decay rate is proportional to

$$\frac{1}{\tau_s} \propto V_0^2\gamma^2(k_zk'_- - k_-k'_z)(k_zk'_+ - k_+k'_z) \propto \gamma^2k_f^4\frac{1}{\tau_p} \tag{B.15}$$

where $1/\tau_p$ is proportional to the V_0^2. Eq. B.15 is equivalent to the Elliott spin relaxation time we obtain from the projected Hamiltonian to the conduction band.

B.2 How the e-e interaction vanishes in calculating the charge conductivity

When derive the quantum kinetic equation, the collision integral contains all kinds of momentum scattering potential especially the e-e interaction. However as we know that when calculating the conductivity, the e-e interaction should vanish int this case. In this appendix, we show that how the e-e interaction naturally vanish in calculating the conductivity. To simplify our discussion, we start from the classical Boltzmann equation without SOC

$$\begin{aligned} & \partial_T f_{k_1} + \frac{1}{2}\{\hat{\mathbf{V}}_k, \cdot \nabla_{\mathbf{R}} f_{k_1}\} - e\mathbf{E}\cdot\nabla_k f_{k_1} = \int U_{k_1,k_1'}(f_{k_1} - f_{k_1'}) \\ + & \int d^n k_1' k_1, d^n k_2' W(k_1, k_1', k_3, k_4) \times \\ & \left[f(k_1)f(k_2)(1-f(k_1'))(1-f(k_2')) - f(k_1')f(k_2')(1-f(k_1))(1-f(k_2))\right], \end{aligned} \tag{B.16}$$

where n is the dimension of the system, f(k) is the Fermi distribution function, $U_{k_1,k_1'}$ is the impurity scattering rate and $W(k_1, k_1'; k_2, k_2')$ is the e-e scattering rate. If we

exchange f_1, f_2 and f_1', f_2', the right hand side of Eq. B.16 is unchanged. This means the electron 2 satisfy the same Boltzmann equation to electron 1 as

$$\begin{aligned}
&\partial_T f_{k_2} + \frac{1}{2}\{\hat{\mathbf{V}}_k, \cdot \nabla_{\mathbf{R}} f_{k_2}\} - e\mathbf{E}\cdot\nabla_k f_{k_2} = \int V(f_{k_2} - f_{k_2'}) \\
+ \quad &\int d^n k_1' d^n k_2 d^n k_2' W(k_1, k_2, k_3, k_4) \times \\
&\left[f(k_1)f(k_2)(1-f(k_1'))(1-f(k_2')) - f(k_1')f(k_2')(1-f(k_1))(1-f(k_2))\right],
\end{aligned} \tag{B.17}$$

The charge current operator is defined as

$$J = \int d^n k_1 (-e\frac{k_1}{m^*} f(k_1) = \int d^n k_2 - e\frac{k_2}{m^*} f(k_2), \tag{B.18}$$

where m^* is the effective electron mass. As we are interested in the DC conductivity, the system is uniform and independent on time. Therefore the first two terms on the left side of Boltzmann equation are zero. To get the charge current equation from the Boltzmann equation, we multiply the charge current operator on the both sides of Eq. B.16 and Eq. B.17 which gives

$$\begin{aligned}
&\int dk_1 \frac{e^2 \boldsymbol{k}_1}{m} \boldsymbol{E}\cdot\boldsymbol{\partial}_{\boldsymbol{k}} f_1 = \int dk_1 dk_1' \frac{-e\boldsymbol{k}_1}{m} U(k_1, k_1')(f_1 - f_1') \\
&+ \int dk_1 dk_2 dk_1' dk_2' \frac{e\boldsymbol{k}_1}{m} W(k_1, k_2, k_1', k_2') \\
&(f_1 f_2 (1-f_1')(1-f_2') - f_1' f_2' (1-f_1)(1-f_2)).
\end{aligned} \tag{B.19}$$

$$\int dk_2 \frac{e^2 \boldsymbol{k}_2}{m} \boldsymbol{E} \cdot \boldsymbol{\partial}_{\boldsymbol{k}} f_2 = \int dk_2 dk_2' \frac{-e\boldsymbol{k}_2}{m} U(k_2, k_2')(f_2 - f_2')$$
$$+ \int dk_1 dk_2 dk_1' dk_2' \frac{e\boldsymbol{k}_2}{m} W(k_1, k_2, k_1', k_2')$$
$$\times \left(f_1 f_2 (1 - f_1')(1 - f_2') - f_1' f_2' (1 - f_1)(1 - f_2)\right). \tag{B.20}$$

The left hand side of Eq. B.19 and Eq. B.20 have the form

$$\begin{aligned} \int dk_{12} \frac{e^2 k_{1(2)}}{m} \boldsymbol{E} \cdot \boldsymbol{\partial}_{\boldsymbol{k}} f_{1(2)} &= \int dk_{1(2)} \boldsymbol{\partial}_{\boldsymbol{k}} \cdot (\frac{e^2 \boldsymbol{k}_{1(2)}}{m} \boldsymbol{E} f_{1(2)}) - \int dk_{1(2)} (\boldsymbol{\partial}_{\boldsymbol{k}} \frac{e^2 \boldsymbol{k}_{1(2)}}{m}) \boldsymbol{E} f_{1(2)} \\ &= \frac{ne^2}{m}, \end{aligned} \tag{B.21}$$

where n is the density of the electron and $j = \int dk \frac{ek}{m} f(k)$ is the electric current. The first term on the right hand side of Eq. B.19 and Eq. B.20 is corresponding to the impurity scattering and equal to $\frac{j}{\tau_{imp}}$ where τ_{imp} is the momentum scattering time due to the impurity. The second term on the right hand side is not easy to be calculated because the momentums k_1, k_2, k_1' and k_2' are not independent but correlated by the fact that the e-e interaction conserve the net momentum which means $k_1 + k_2 = k_1' + k_2'$. However, if we calculate $\frac{1}{2}(Eq.B.19 + Eq.B.20)$, the e-e scattering can be written as

$$\int dk_1 dk_2 dk_1' dk_2' \frac{e(\boldsymbol{k}_1 + \boldsymbol{k}_2)}{2m} W(k_1, k_2, k_1)', k_2')$$

$$\begin{aligned} \times \quad & (f_1 f_2 (1-f_1')(1-f_2') - f_1' f_2' (1-f_1)(1-f_2)) \\ = \quad & \int dk_1 dk_2 dk_1' W(k_1, k_2; k_1', k_2') \qquad \text{(B.22)} \\ & \times (\frac{e(\boldsymbol{k}_1 + \boldsymbol{k}_2)}{2m} f_1 f_2 (1-f_1')(1-f_2') - \frac{e(\boldsymbol{k}_1' + \boldsymbol{k}_2')}{2m} f_1' f_2' (1-f_1)(1-f_2)) \\ = \quad & 0. \qquad \text{(B.23)} \end{aligned}$$

Therefore the charge current equation, $\frac{1}{2}(Eq.B.19 + Eq.B.20)$, has the form

$$\frac{ne^2}{m} = \frac{j}{\tau_{imp}}, \qquad \text{(B.24)}$$

where e-e scattering term exactly disappear in this current equation as long as the e-e interaction conserves the net momentum which is not sensitive to the form of the e-e scattering rate $W(k_1, k_1'; k_2, k_2')$. However, when deriving the density equation, we need not multiply the current operator and therefore e-e scattering can not be canceled as we did in the current equation. This is reasonable because the density does not care about the net momentum which is the key to get the current equation. Therefore although the original Boltzmann equation of the distribution function contains the e-e interaction, the electron-electron scattering will disappear when we calculate the conductivity. However, when calculating the density equation, we need not multiply the current operator on the Boltzmann equation and the This means

the e-e interaction will not affect the conductivity but can contribute the density diffusion.

B.3 The derivation of the matrix element of the spin dynamic equation

The denominator of Eq. 3.36 can be expand to

$$\begin{aligned} & \frac{1}{\tilde{\Omega}^2 + 4k^2\tau^2\cos^2\theta\lambda_1^2 + 4k^2\tau^2\sin^2\theta\lambda_2^2} \\ \approx\ & 1 + 2i\tilde{\omega} - 2i(\tilde{q}_x\cos\theta + \tilde{q}_y\sin\theta) - 3\tilde{q}_x^2\cos^2\theta - 3\tilde{q}_y^2\cos^2\theta \\ & -4k^2\tau^2\cos^2\theta\lambda_1^2 - 4k^2\tau^2\sin^2\theta\lambda_2^2, \end{aligned} \tag{B.25}$$

where $\tilde{\omega} = \omega\tau$ and $\tilde{q}_{x(y)} = q_{x(y)}v\tau$. Substituting Eq. B.25 to Eq. 3.28 we have

$$\begin{aligned} D_{13} &= -D_{31} = \int \frac{d\theta}{2\pi} \frac{2\lambda_1 k\tau\cos\theta}{\tilde{\Omega}^2 + 4k^2\tau^2\cos^2\theta\lambda_1^2 + 4k^2\tau^2\sin^2\theta\lambda_2^2} \\ &\approx -\int \frac{d\theta}{2\pi} 4ik\tau\tilde{q}_x(\alpha + \beta_1 - 2\beta_3\cos 2\theta)\cos^2\theta = -2i(\alpha + \beta_1 - \beta_3)k\tau\tilde{q}_x \end{aligned} \tag{B.26}$$

$$\begin{aligned} D_{23} &= -D_{32} = \int \frac{d\theta}{2\pi} \frac{-2\lambda_2 k\tau\sin\theta}{\tilde{\Omega}^2 + 4k^2\tau^2\cos^2\theta\lambda_1^2 + 4k^2\tau^2\sin^2\theta\lambda_2^2} \\ &\approx \int \frac{d\theta}{2\pi} 4ik\tau\tilde{q}_y(\beta_1 - \alpha_1 + \beta_3\cos 2\theta)\sin^2\theta = 2i(\beta_1 - \beta_3 - \alpha)k\tau\tilde{q}_y \end{aligned} \tag{B.27}$$

$$
\begin{aligned}
D_{33} &= \int \frac{d\theta}{2\pi} \frac{\tilde{\Omega}}{\tilde{\Omega}^2 + 4k^2\tau^2\cos^2\theta\lambda_1^2 + 4k^2\tau^2\sin^2\theta\lambda_2^2} \\
&\approx \int \frac{d\theta}{2\pi}(1 + i\tilde{\omega} - \tilde{q}_x^2\cos^2\theta - \tilde{q}_y^2\sin^2\theta - 4k^2\tau^2\cos^2\theta\lambda_1^2 - 4k^2\tau^2\sin^2\theta\lambda_2^2) \\
&= 1 + i\tilde{\omega} - \frac{1}{2}(\tilde{q}_x^2 + \tilde{q}_y^2) - 4(\alpha^2 + (\beta_1 - \beta_3)^2 + \beta_3^2)k^2\tau^2 \\
&= 1 + i\tilde{\omega} - \frac{1}{2}(\tilde{q}_x^2 + \tilde{q}_y^2) - \tilde{\Omega}_{so}^2\tau^2,
\end{aligned}
\tag{B.28}
$$

$$
\begin{aligned}
D_{11} &= \int \frac{d\theta}{2\pi} \frac{\tilde{\Omega}^2 + 4\lambda_2^2k^2\tau^2\sin^2\theta}{\tilde{\Omega}(\tilde{\Omega}^2 + 4k^2\tau^2\cos^2\theta\lambda_1^2 + 4k^2\tau^2\sin^2\theta\lambda_2^2)} \\
&\approx D_{33} + \int \frac{d\theta}{2\pi} 4\lambda_2^2k^2\tau^2\sin^2\theta = D_{33} + (\frac{1}{2}(\alpha - \beta_1)^2 + (\alpha - \beta_1)\beta_3 + \beta_3^2)4k_F^2\tau^2 \\
&= 1 + i\tilde{\omega} - \frac{1}{2}(\tilde{q}_x^2 + \tilde{q}_y^2) - 2(\alpha^2 + (\beta_1 - \beta_3)^2 + \beta_3^2)k^2\tau^2 - \alpha(\beta_1 - \beta_3) \\
&= 1 + i\tilde{\omega} - \frac{1}{2}(\tilde{q}_x^2 + \tilde{q}_y^2) - \frac{1}{2}\Omega_{so}^2\tau^2 4k_F^2\tau^2\alpha(\beta_1 - \beta_3)
\end{aligned}
\tag{B.29}
$$

$$
\begin{aligned}
D_{22} &= \int \frac{d\theta}{2\pi} \frac{\tilde{\Omega}^2 + 4\lambda_2^2k^2\tau^2\sin^2\theta}{\tilde{\Omega}^2 + 4k^2\tau^2\cos^2\theta\lambda_1^2 + 4k^2\tau^2\sin^2\theta\lambda_2^2} \\
&\approx \int \frac{d\theta}{2\pi}(1 + i\tilde{\omega} - \tilde{q}_x^2\cos^2\theta - \tilde{q}_y^2\sin^2\theta - 4k^2\tau^2\cos^2\theta\lambda_1^2) \\
&= 1 + i\tilde{\omega} - \frac{1}{2}(\tilde{q}_x^2 + \tilde{q}_y^2) - 2(\alpha^2 + (\beta_1 - \beta_3)^2 + \beta_3^2)k^2\tau^2 + \alpha(\beta_1 - \beta_3) \\
&= 1 + i\tilde{\omega} - \frac{1}{2}(\tilde{q}_x^2 + \tilde{q}_y^2) - \frac{1}{2}\Omega_{so}^2\tau^2 + 4k^2\tau^2\alpha(\beta_1 - \beta_3)
\end{aligned}
\tag{B.30}
$$

where $\Omega_{so} = 2\sqrt{\alpha^2 + (\beta_1 - \beta_3)^2 + \beta_3^2}k$.

VITA

Name: Xin Liu

Address: Department of Physics

Texas A&M University

College Station, TX, 77843-4242

Email Address: liuxin@physics.tamu.edu

Education: B.S. College of Physics, Nankai University, China, 2003

M.S. Chern Institute of Mathematics, China, 2006